An Empirical Model for attributing sources of particulate matter

PK Davy WJ Trompetter

GNS Science Report 2020/33
November 2020

DISCLAIMER

The Institute of Geological and Nuclear Sciences Limited (GNS Science) and its funders give no warranties of any kind concerning the accuracy, completeness, timeliness or fitness for purpose of the contents of this report. GNS Science accepts no responsibility for any actions taken based on, or reliance placed on the contents of this report and GNS Science and its funders exclude to the full extent permitted by law liability for any loss, damage or expense, direct or indirect, and however caused, whether through negligence or otherwise, resulting from any person's or organisation's use of, or reliance on, the contents of this report.

BIBLIOGRAPHIC REFERENCE

Davy PK, Trompetter WJ. 2020. An Empirical Model for attributing sources of particulate matter. Lower Hutt (NZ): GNS Science. 49 p. (GNS Science report; 2020/33). doi:10.21420/ H7NX-HM56.

PK Davy, GNS Science, PO Box 30368, Lower Hutt 5040, New Zealand
WJ Trompetter, GNS Science, PO Box 30368, Lower Hutt 5040, New Zealand

www.gns.cri.nz

ISSN 2350-3424 (online)
ISBN 978-1-99-001055-2 (online)
http://dx.doi.org/10.21420/ H7NX-HM56

CONTENTS

FIGURES

TABLES

APPENDICES

APPENDIX FIGURES

ABSTRACT

Airborne particulate matter (PM) pollution is well-known to have significant adverse effects on human health. It also has a range of environmental effects, including local reductions in visibility, effects on the radiative balance and deposition of contaminated material onto land and waterways. Because of these effects, PM concentrations are routinely monitored in numerous countries and managed according to local legislation.

In New Zealand, the National Environmental Standard (NES) for PM sets a 24-hour average limit for PM_{10} (particulate matter with aerodynamic diameters less than 10 µm) concentrations at 50 µg m^{-3} with regulatory authorities required to report exceedances and manage air quality to reduce pollution concentrations. Many urban areas in New Zealand exceed the NES repeatedly each year, particularly during the winter when wood combustion is used as a source of energy for home heating. Understanding the sources of air pollution and their relative contribution to total PM concentrations is therefore important for managing air quality to reduce the health impacts for exposed populations.

The National Air Particulate Matter Speciation Database (NAPMSD) held by the Institute of Geological and Nuclear Sciences (GNS Science), contains air particulate matter compositional data for samples collected since 1998 at various New Zealand urban air quality monitoring sites. The particulate matter composition data has been used to identify the sources and how much they contribute to PM pollution concentrations at those locations. This quantitative source contribution data has been used to construct and test an empirical model to help define source contributions at those locations where particulate matter concentration monitoring data ($PM_{2.5}$ and PM_{10}) is available but there is no breakdown by source contributions. The delineation of source contributions to total particulate matter concentrations is useful to inform both regional and national policy to mitigate the health and socio-economic effects of air pollution in New Zealand. The empirical model was found to reproduce the peak winter contributions from biomass combustion (wood burning) for residential space heating when compared to the source apportionment data for the same locations. The results are such that there is confidence that the empirical model can be used to estimate monthly and annual average contributions at those locations where $PM_{2.5}$ and PM_{10} concentration monitoring data is available (but no breakdown by source) for use in health effects studies or assessing winter particulate matter concentration trends.

KEYWORDS

Air particulate matter, source apportionment, empirical model, biomass combustion

1.0 INTRODUCTION

Since 1998 the Institute of Geological and Nuclear Sciences (GNS Science) has used an air particulate matter (PM) composition analysis and receptor modelling approach to identify sources (including natural sources) of airborne particles in New Zealand airsheds. This work has been conducted primarily on behalf of Regional Councils seeking to understand the sources that lead to air pollution episodes so that air quality can be managed to protect human health as required by the National Environmental Standards for Air Quality[1]. The data that has been collected over the years has been compiled into the National Air Particulate Matter Speciation Database (NAPMSD) held by GNS Science. The NAPMSD contains air particulate matter compositional data for a subset New Zealand towns and cities that has been used to identify the sources contributing to particulate matter pollution at those locations. The particulate matter compositional data held by GNS Science have been generated consistently using internationally accepted methodologies (USEPA) and quality assurance procedures with traceable standards including successful participation in international inter-laboratory comparisons (Hyslop et al. 2019, Yatkin et al. 2020). The elemental concentrations in filter-based particulate matter samples have been determined by Ion Beam Analysis (IBA) and/or X-ray fluorescence (XRF) at the New Zealand National Isotope Centre.

This report presents an analysis of data from the NAPMSD for the composition and sources of airborne particulate matter samples collected at air quality monitoring sites around New Zealand. In particular, the focus of this work was on developing an empirical model for disaggregating the source contributions to urban PM concentrations for those locations where no composition and source apportionment data was available. The delineation of source contributions to total airborne particulate matter concentrations is useful to assess population exposure for epidemiological health effects research (such as the current HAPINZ 3.0[2] study) designed to inform both regional and national policy aimed at mitigating the health and socio-economic impacts of air pollution in New Zealand. The report describes the methodology used to derive the empirical source attribution model, any sensitivities and limitations in the model, and compares the results to those obtained from actual source contribution data from receptor modelling studies.

[1] Resource Management (National Environmental Standards for Air Quality) Regulations 2004 (SR 2004/309) Reprint as at 1 September 2020 available at
http://www.legislation.govt.nz/regulation/public/2004/0309/latest/DLM286835.html

[2] Health and air pollution in New Zealand 3.0 (2021) in preparation for Ministry for the Environment, Waka Kotahi NZ Transport Agency and Ministry of Transport.

2.0 PARTICULATE MATTER MONITORING SITES IN NEW ZEALAND

Filter based particulate matter (PM) samples have been collected and analysed since 1996 for approximately 40 sites across New Zealand, with some urban areas including multiple sites (Figure 2.1). The majority of particulate matter sampling and analysis campaigns have been targeted studies commissioned by regional councils that ran for 1–2 years collecting 24-hour time integrated particulate matter samples in order to better understand the local drivers of air pollution for air quality management purposes. The exception to this is the Auckland Council multi-site air particulate matter speciation database that has been running since mid-2004 which allows for inter-site comparisons, trend analysis and all-of-urban assessment of PM composition and source contributions to both $PM_{2.5}$ and PM_{10} particulate matter size fractions.

In addition to the urban monitoring locations, several studies have targeted source specific particulate matter composition, these include motor vehicle tunnels (Mt Victoria tunnel, Wellington and the Johnstone Hill Tunnel north of Auckland) (Ancelet et al. 2011a, Davy et al. 2011a) and wood burner emissions (Davy et al. 2009, Ancelet et al. 2010, Ancelet et al. 2011b) in order to better understand emission source characteristics and composition. For several locations, high-resolution sampling (hourly) and analysis was undertaken as part of research programmes[3] to understand the observed diurnal variation in particulate matter concentrations in New Zealand urban centres (Ancelet et al. 2012, Ancelet et al. 2014b, Ancelet et al. 2014a, Trompetter et al. 2010) as well as the impacts of infiltration and ventilation on indoor air quality (Trompetter and Davy 2019).

Figure 2.1 Urban particulate matter speciation sampling locations in New Zealand.

[3] MBIE Contract C05X0903 2009–2012: Understanding air particulate matter pollution? *Sources, patterns and transport of air particulate matter in polluted New Zealand urban environments*
BRANZ Contract LR0515 2017–2018 *Warmer, drier, healthier buildings: exploring the indoor environment in schools and homes,*

As a result, GNS Science holds an archive of filter-based, time-integrated particulate matter samples that have been analysed gravimetrically to provide ambient particulate matter concentrations, then by appropriate analytical techniques to provide elemental composition data. The particulate matter compositional data has been derived from particulate matter samples collected at regulatory authority monitoring sites using National Environmental Standards for Air Quality (NESAQ) compliant methodologies or alongside NESAQ compliant particulate matter monitoring systems. The PM compositional data has been used to determine source contributions to ambient PM concentrations by receptor modelling techniques.

2.1 Analysis of Particulate Matter Composition

Two multi-elemental analysis techniques have been used routinely to provide the particulate matter composition analysis, these are accelerator-based ion beam analysis (IBA) and X-ray fluorescence analysis (XRF), while light reflectance has been used to determine Black Carbon (BC) concentrations in all samples. These are well established and internationally accepted methods for determining PM elemental composition (Horvath 1993, Landsberger and Creatchman 1999, Maenhaut and Malmqvist 2001, Bond and Bergstrom 2006). Full descriptions of these techniques are provided in Appendix 1. IBA and XRF are both non-destructive analytical techniques and provide complimentary elemental results where XRF is more sensitive (lower limits of analytical detection) for heavier elements, particularly heavy metals, and IBA is more sensitive for lighter elements (Na to K) with the ability to determine hydrogen concentrations, a useful marker for hydrocarbon and secondary aerosol species.

GNS Science has used the accelerator based IBA techniques to measure elemental concentrations in New Zealand particulate matter samples since 1996, then in 2013 the analysis capability was extended by acquiring the XRF analytical facility (Epsilon 5, Panalytical Pty, Netherlands).

2.2 Receptor Modelling of Particulate Matter Composition

The multivariate analysis of air particulate matter sample composition (also known as receptor modelling or source apportionment) provides groupings (or factors) of elements that vary together over time. This technique effectively ‘fingerprints’ the sources that are contributing to airborne particulate matter concentrations and the mass of each element (including BC) attributed to that source. Most commonly used receptor models are based on conservation of mass from the point of emission to the point of sampling and measurement (Hopke 1999). Their mathematical formulations express ambient chemical concentrations as the sum of products of species abundances in source emissions and source contributions. In other words, the chemical composition of filter-based samples of particulate matter collected at a monitoring station is resolved mathematically to be the sum of a number of different factors or sources of those particles.

GNS Science has used the receptor modelling approach to identify sources of particulate matter in New Zealand airsheds by applying a technique known as Positive Matrix Factorisation (PMF) analysis to particulate matter composition data (Paatero and Tapper 1994, Hopke et al. 1999). A direct result of using this technique is that the sources of particulate matter (or any other variable) were also derived and the mass contribution of each emission source to atmospheric concentrations was determined. Appendix 2 identifies the specific sampling sites, sampling period and reporting details that included PM elemental speciation, receptor modelling and reporting.

2.3 Contributions of Emission Sources to Urban Particulate Matter

Receptor modelling studies for New Zealand locations (Davy et al. 2016, Davy and Trompetter 2017a, Davy and Trompetter 2017b, Davy and Trompetter 2018, Davy and Trompetter 2019) have shown that, at urban locations, there are generally five main sources contributing to ambient particulate matter concentrations:

1. Motor vehicles (tailpipe and non-engine emissions)
2. Biomass combustion (mainly residential wood burning for winter space heating)
3. Secondary aerosol from gas-to-particle atmospheric reactions which is generally dominated by secondary sulphate aerosol
4. Marine aerosol (sea salt) generated in the oceans
5. Crustal matter (soil) from local

Sources additional to those listed above do contribute to ambient urban concentrations but the relative contribution from a particular source depends on local emissions activity and, for receptor modelling analysis, the location of a monitoring site.

2.3.1 Transport Emissions

Emissions to atmosphere from the transport sector has a significant impact on particulate matter concentrations in urban areas. The transport sector is associated with multiple emission sources of PM, including:

- tailpipe emissions from the combustion of fuels (petrol and diesel vehicles);
- re-suspended dusts and particles (collectively known as road dust) from the road surface, tyres, brake wear and other mechanical abrasion processes;
- emissions of particulate matter from ships' engines; and
- secondary particle formation from gas-to-particle atmospheric reactions of combustion-related gases (e.g. sulphur dioxide gas produced from the combustion of sulphur-containing fuels will react to form secondary sulphate particles some way downwind depending on temperature, relative humidity and insolation).

There are key differences in particle size and composition for the various transport sector emission sources. Tailpipe emissions of particles from fuel combustion are primarily less than 2.5 μm (μm = microns = 10^{-6} m), with most in the ultra-fine size range (<0.1 μm), whereas the road dust component is dominated by larger particles between 2.5 μm and 10 μm ($PM_{10-2.5}$) generated by mechanical abrasion processes. A key factor in the contribution of motor vehicles to ambient particulate matter concentrations on an area basis (for exposure assessment) was the proximity to roadways and the traffic volumes and density of the local urban network. (Davy and Trompetter 2019).

2.3.2 Biomass Combustion

Mass contributions from biomass combustion were found to be present at all sites where monitoring included the winter period when peak concentrations from this source occur. Particles from biomass combustion sources are primarily less than 2.5 μm. The biomass combustion source represents the combustion of all plant material and the peak winter concentrations are primarily due to wood combustion in solid fuel appliances used for domestic heating. Mass contributions from biomass combustion sources vary from year to year

depending on climate conditions with colder, calmer conditions leading to peak urban concentrations.

2.3.3 Natural Sources of Airborne Particulate Matter

One of the key results from receptor modelling analyses is the derivation of mass contributions to ambient aerosol concentrations from natural sources and sources for which little useful information is available from other methods of source apportionment such as emissions inventories. The information is vital for air quality management as the proportion of particle mass from natural and other (uncontrollable) sources needs to be factored into any air pollution reduction strategy. A straightforward definition of natural sources of particulate matter is that the source can only be considered 'natural' if it involves no direct or indirect human activity[4]. For example, particulate matter pollution from a wildfire can only be considered natural if it was ignited by lightening or similar. If the fire was due to accidental or deliberate human activity as the ignition source, then it is considered as an anthropogenic source.

The New Zealand datasets show that oceanic or marine aerosol (sea salt) is the primary source of natural aerosol present in New Zealand urban atmospheres. Secondary sulphate aerosol formed from gas-to-particle atmospheric reactions has both natural (oceanic phytoplankton, volcanic emissions) and anthropogenic (combustion of sulphur containing fuels, industrial emissions) gaseous precursor sources. The third component of urban PM that has natural origins is crustal matter, generally referred to as ‘Soil’ in source apportionment studies. However, time-variation analyses across multiple datasets (see Section 2.3.3.3) show that urban Soil PM concentrations are lower on weekends than weekdays indicating that the generation of airborne crustal matter in urban locations is largely the result of human activities (construction/demolition, earthworks, roadworks, passage of vehicles on roads and unpaved areas) and therefore does not meet the ‘natural source’ criteria discussed above. The following sections provide further detail on each of these sources.

2.3.3.1 Marine Aerosol

Sodium and chlorine are the primary constituents of marine aerosol (or sea salt) and were also significant elemental contributors to both $PM_{2.5}$ and PM_{10} mass at New Zealand monitoring sites along with the more minor components (K, Ca, Mg, S) of sea salt. The elements were highly correlated (as shown for the Auckland dataset in Figure 2.2) and present in the same ratio at peak concentrations as found in sea salt ([Na] = 0.56[Cl]) (Lide 1992). The analytical results demonstrate the relative influence of this natural aerosol source on urban particulate matter concentrations in New Zealand, even for inland locations, due to the isolated oceanic location of the New Zealand landmass. The marine aerosol component of urban air particulate matter is considered to be part of the ‘natural’ background and therefore is that proportion that cannot be managed.

[4] *Particulate matter from natural sources and related reporting under the EU Air Quality Directive in 2008 and 2009*. Technical report No. 10/2012. European Union 2012
https://www.eea.europa.eu/publications/particulate-matter-from-natural-sources

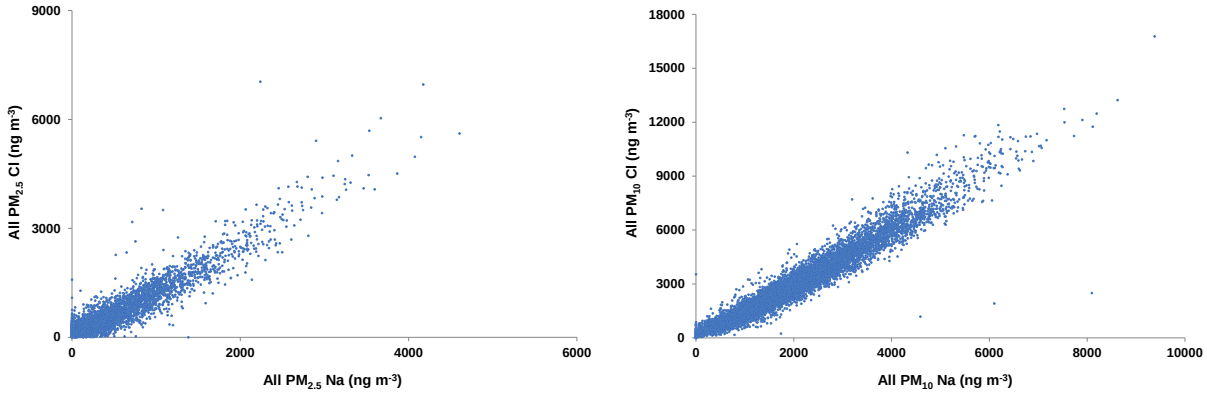

Figure 2.2 Scatterplots for sodium and chlorine in $PM_{2.5}$ (left) and PM_{10} (right) for all Auckland PM samples.

Research has shown that the concentration of marine aerosol shows a strong dependence on wind speed across the ocean surface and ranges from about 2 µg m^{-3} to as much as 50 µg m^{3} or more at wind speeds in excess of 15 m s^{-1} (Fitzgerald 1991) and the Auckland data corroborates those potential concentration ranges. Therefore, marine aerosol concentrations in New Zealand urban areas are largely influenced by meteorological and long-range transport mechanisms (Davy et al. 2011b). This long-range transport process results in relatively uniform marine aerosol concentrations in a regional airmass. For example, marine aerosol concentrations at the central Auckland Queen Street site were found to be well correlated with those at the background site at Patumahoe 40 km southwest of the Auckland CBD as presented in Figure 2.3 (Davy and Trompetter 2019).

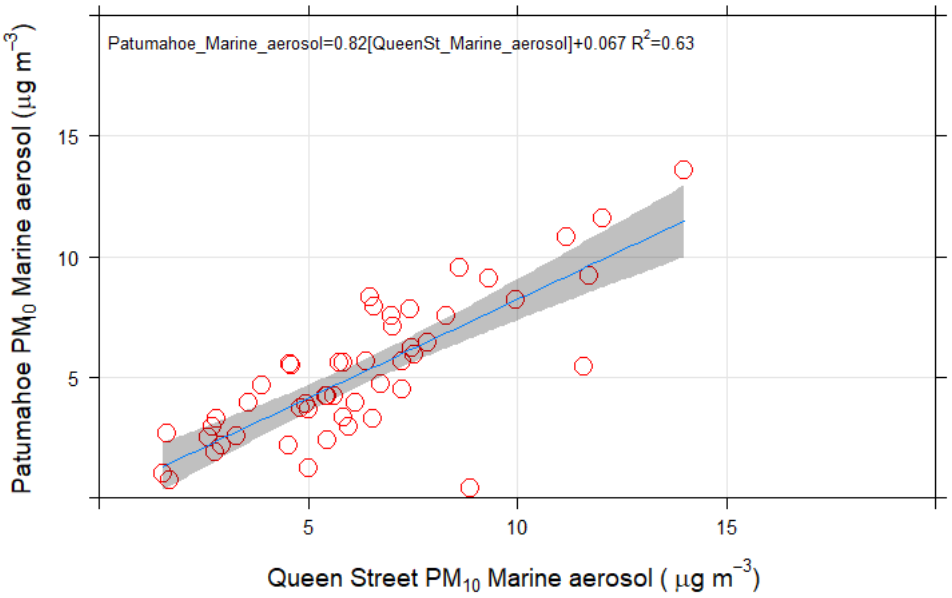

Figure 2.3 Plot of marine aerosol concentrations in PM_{10} at Queen Street versus Patumahoe during 2010.

Similarly, further south, marine aerosol concentrations were found to be homogenous across the Nelson and Tasman airsheds as shown in Figure 2.4 (Ancelet et al. 2013).

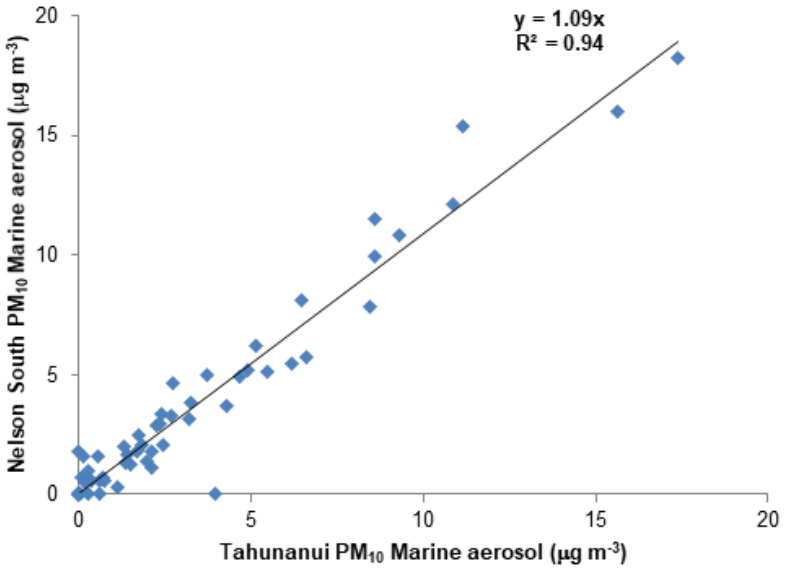

Figure 2.4 Plot of marine aerosol concentrations in PM_{10} at Nelson City and Tahunanui during 2009.

The primary influence on the regional concentrations of marine aerosol appears to be the relative exposure to prevailing oceanic winds and the sheltering effect of mountain and hill ranges most likely due to impaction and orographic rain-out. Figure 2.5 presents marine aerosol concentration data derived from source apportionment studies (> 1 year) across New Zealand. Note that the Awatoto (Hawkes Bay) site was immediately adjacent the ocean.

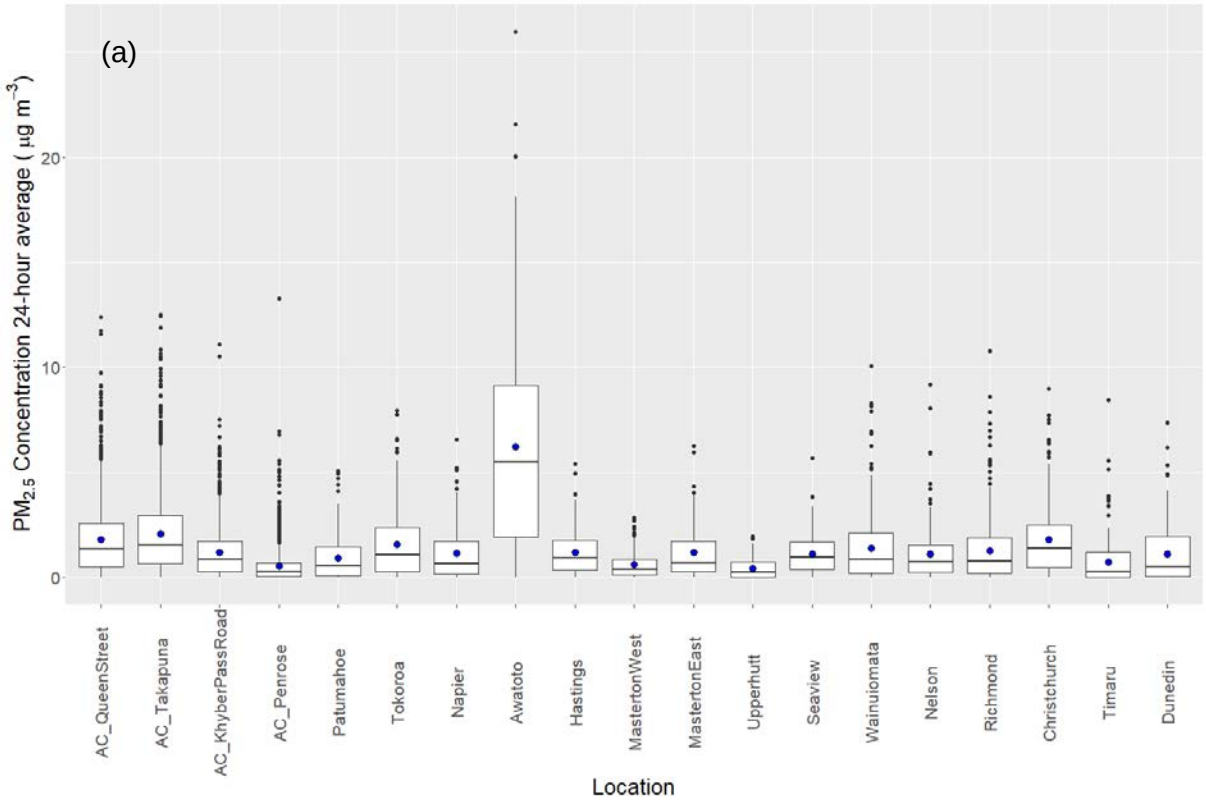

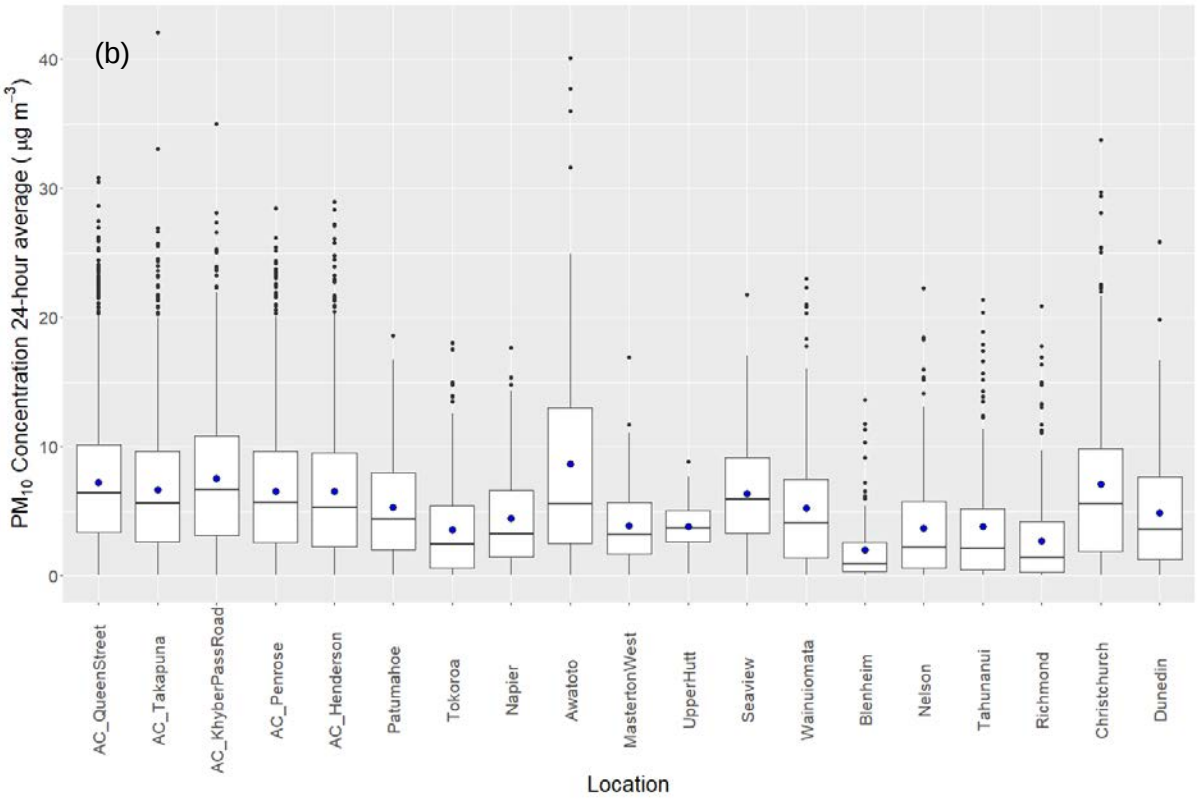

Figure 2.5 Box and whisker plot of (a) $PM_{2.5}$ and (b) PM_{10} marine aerosol concentrations across New Zealand.

2.3.3.2 Secondary Sulphate Aerosol

The presence of sulphur in airborne particulate matter is generated from a variety of sources including sulphur incorporated in mineral structures of crustal matter, cell structure of trees (released during biomass combustion), volcanic emissions, marine aerosol, and the combustion of sulphur containing fuels including automotive fuels (petrol, diesel, fuel oils used by ships) and other fossil fuels such as coal. Sulphur containing particulate matter is also derived from precursor gases such as sulphur dioxide, hydrogen sulphide or dimethyl sulphide from the gas-to-particle reaction process in the atmosphere. These reactions can take hours to days depending on the reaction pathway followed, the availability of catalytic metals (e.g. Fe, Mn), relative humidity and the strength of solar radiation (Seinfeld and Pandis 2006). Therefore, concentrations of sulphur containing particulate matter from secondary sulphate sources are likely to be highest some distance downwind of a precursor gas emission source (Polissar et al. 2001). Seasonal patterns show that secondary sulphate concentrations generally have a summer maximum and a winter minimum (Figure 2.6), reflecting the relative influence of solar forcing on atmospheric reaction pathways.

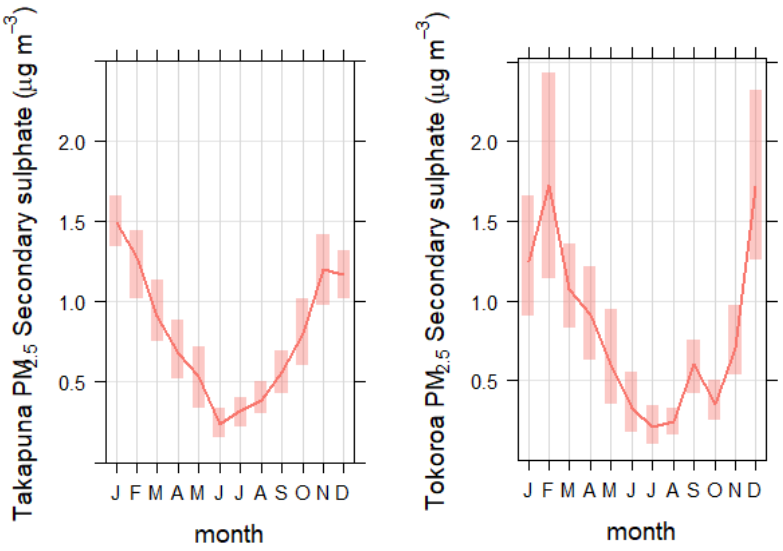

Figure 2.6 Seasonal variation in secondary sulphate concentrations at (left) Takapuna, Auckland (2006–2013) and (right) Tokoroa, Waikato (2016).

The New Zealand source apportionment data indicates that there are both natural (oceanic, volcanic) and anthropogenic (shipping, motor vehicle and industrial emissions) sources of secondary sulphate aerosol. The relative contribution secondary sulphate particles to PM concentrations at a given air quality monitoring site is dependent on:

- local source precursor gas emission activity (both anthropogenic and natural),
- the proximity of a PM sampling site to such activities,
- atmospheric chemical reaction kinetics (i.e. the drivers for the gas-to-particle reaction pathway) and;
- the long-range transport of natural source (volcanic and oceanic) secondary sulphate.

Receptor modelling studies of PM composition from around New Zealand show that PM monitoring sites near ports are likely to be influenced by secondary sulphate associated with emissions of precursor gases from ships engines. Also, some monitoring locations were influenced by direct emissions of combustion-derived particulate matter from ships engines (Davy and Trompetter 2019).

2.3.3.3 Crustal Matter

Crustal matter is primarily composed of aluminosilicate minerals and the source profiles extracted from receptor modelling reflect this, with Al and Si being the primary constituents and Mg, K, Ca, Ti and Fe commonly present. The mass ratio of Si/Al is consistently about 3:1 for both PM_{10} and $PM_{2.5}$ size fractions across all New Zealand monitoring sites and is similar to the Si/Al ratio in aluminosilicate crustal minerals. Aluminium and silicon concentrations were primarily associated with crustal matter (synonymous with Soil as a source reference) which is predominantly a coarse particle source generated by mechanical abrasion of surface material. In urban locations, the passage of motor vehicles over roads can be the primary source of crustal matter suspension and resuspension (Thorpe and Harrison 2008).

A specific dust event that resulted in PM_{10} exceedances across the Auckland region was identified as originating from a dust storm (a natural event) in the Australian desert during September 2009 (Davy et al. 2011b), the influence of which can be seen in the time-series plots for Al and Si in all Auckland PM_{10} samples presented in Figure 2.7.

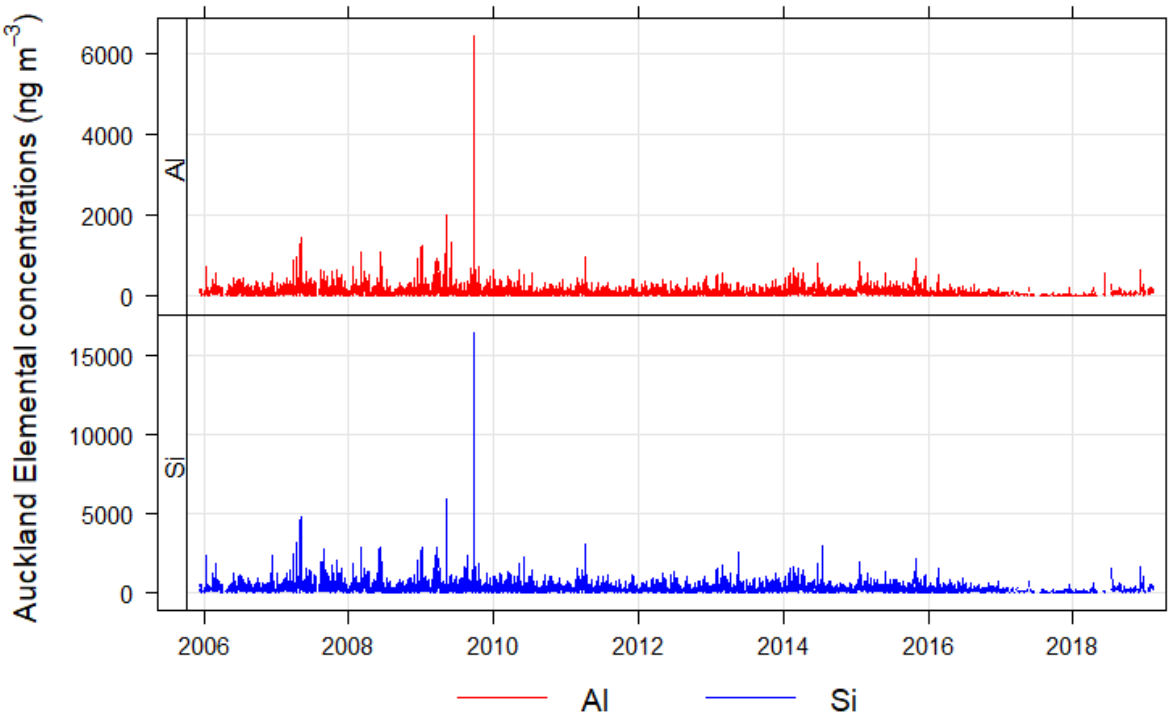

Figure 2.7 Time-series plots for aluminium and silicon in all Auckland PM_{10} samples.

The temporal variation for both aluminium and silicon concentrations indicate that airborne concentrations are primarily from anthropogenic activities because of the day-of-the-week concentration dependence with weekend concentrations significantly lower than weekdays as presented for Auckland data in Figure 2.8. Any randomly generated emissions such as wind-blown dust, would not show a bias for day of the week due to the random nature of meteorological events.

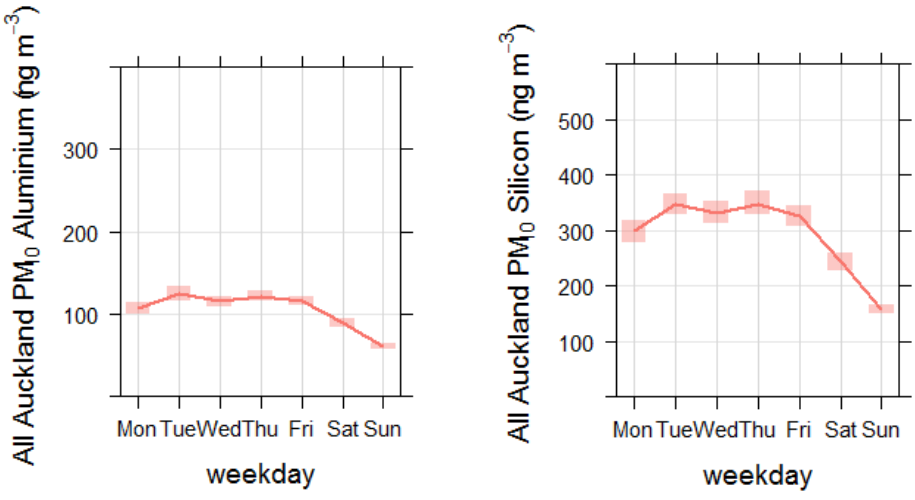

Figure 2.8 Temporal variations in aluminium (left) and silicon (right) in all Auckland PM_{10} samples (the shaded bars are the 95 percentile confidence limits in the mean).

Crustal matter source contributions at the monitoring sites were likely to be a combination of windblown soil, road dust and dust generated by earthworks, construction and road works. Concentrations were found to vary from site to site depending on meteorological conditions and local dust generating activities. Given the clear temporal pattern it is likely that resuspension of crustal matter by the passage of motor vehicles on roads, driveways and unsealed yards is the dominant source of airborne dust in urban settings.

3.0 EMPIRICAL MODEL FOR ATTRIBUTING SOURCES OF PARTICULATE MATTER

The existing particulate matter source apportionment data for NZ towns and cities (Davy and Trompetter 2017b) has been analysed to construct an empirical model for use at those locations where particulate matter concentration monitoring data is available but there is no breakdown by source contributions.

Briefly, the model relies on the fact that peak PM concentrations are observed during winter in New Zealand urban areas as shown for Richmond (Figure 3.1) primarily driven by biomass combustion (domestic fires for space heating) from May to September each year (Figure 3.2).

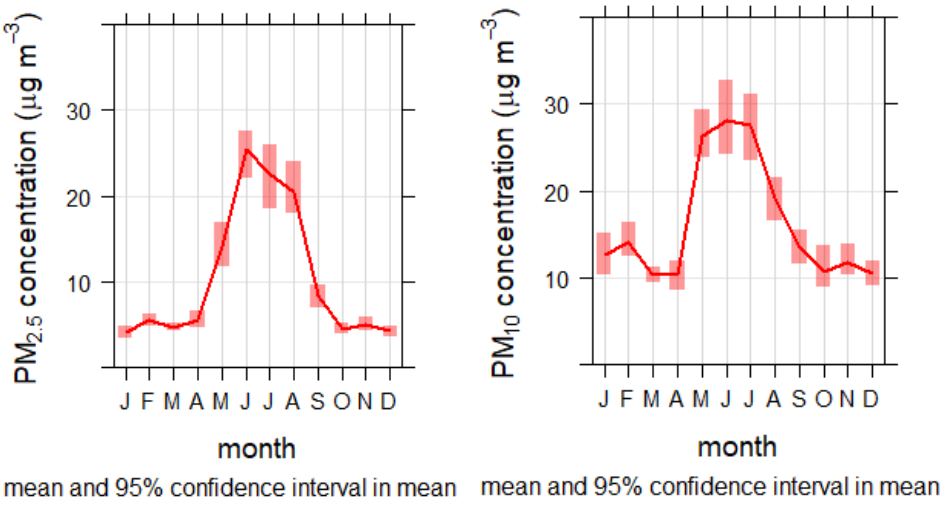

Figure 3.1 Monthly average $PM_{2.5}$ (2016) and PM_{10} (2013 to 2016) at Richmond, Tasman District showing peak winter concentrations.

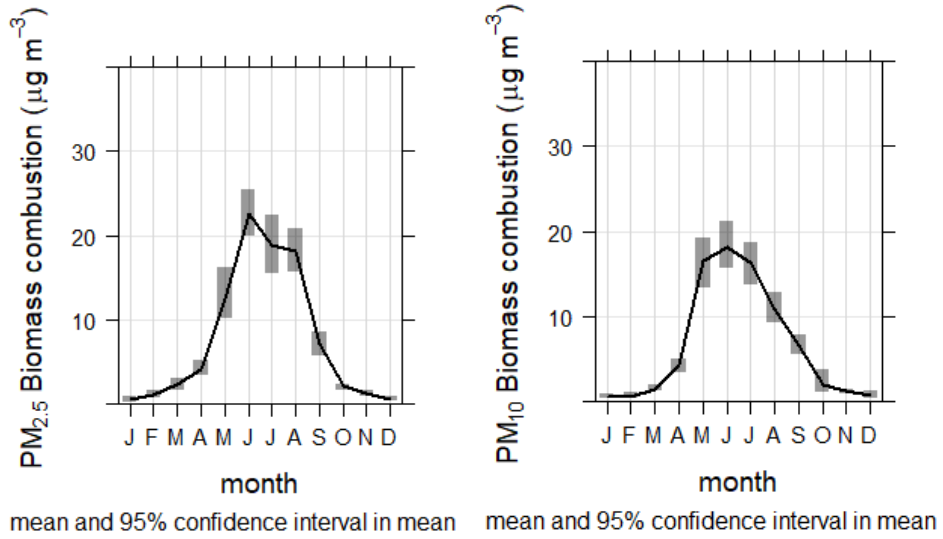

Figure 3.2 Monthly average Biomass combustion source contributions to $PM_{2.5}$ (2016) and PM_{10} (2013 to 2016) at Richmond, Tasman District showing peak winter concentrations.

Natural sources, motor vehicle and other anthropogenic emissions are assumed to be relatively constant all year (Davy and Trompetter 2018). We have then separated the winter, or rather the 'burning season' peak (April to September) PM data and assigned that to biomass combustion sources with the remainder being the combination of motor vehicle emissions, secondary sulphate, crustal matter (soil), marine aerosol (sea salt) and other sources more likely to be specific to a monitoring site. The breakdown of the remainder is relatively simple as there is good regional data for the primary natural sources (sea salt and secondary sulphate). Motor vehicles vehicle contributions are a function of traffic type and density in the area of the monitoring site and are generally a combination of tail pipe emissions ($PM_{2.5}$) and road dust ($PM_{10\text{-}2.5}$) which also largely accounts for crustal matter in urban areas (Davy and Trompetter 2018).

The empirical model is essentially a 'peak to mean' ratio analysis with the average PM concentration during winter (i.e. without a biomass combustion peak) assumed to be the same as for the October to March period. However, this assumed winter average does have an increment subtracted to allow for the observed decrease in secondary sulphate concentrations and some suppression of crustal matter particulate matter during winter due to wetter conditions. Seasonal patterns show that secondary sulphate concentrations generally have a summer maximum and a winter minimum (see Figure 2.6), reflecting the relative influence of oceanic biota production of precursor gases and solar forcing on atmospheric reaction pathways (Davy and Trompetter 2018).

The winter subtraction for $PM_{2.5}$ has been set at -1.5 µg m^{-3} (but -1.0 µg m^{-3} north of the Bombay Hills) and for PM10 it is -3.0 µg m^{-3} (but -1.5 µg m^{-3} north of Bombay Hills). Additionally, due to source contributions from biomass burning at other times of the year the 'summer' months (October to March) have been given a value of 0.5 µg m^{-3} for $PM_{2.5}$ at any location north of the Bombay Hills while for PM_{10} and for both size fractions at all other locations in NZ, the value has been set at 1.0 µg m^{-3}. Appendix 3 provides the generic calculation templates for calculating the empirical model data from $PM_{2.5}$ and PM_{10} monthly average concentration datasets.

The two graphs presented in Figure 3.3 illustrate how the empirical model works for $PM_{2.5}$ and PM_{10} data from Richmond, Tasman District (Davy and Trompetter 2017a). The red trace is the monitored PM data, while the black trace is the biomass combustion, contribution derived from source apportionment by receptor modelling. The blue trace is the difference between these two quantities, i.e. the contribution to $PM_{2.5}$ and PM_{10} from all other sources. The purple trace is the empirical biomass combustion contribution while the yellow trace is the empirical model result for all other sources of particulate matter which can then be disaggregated further.

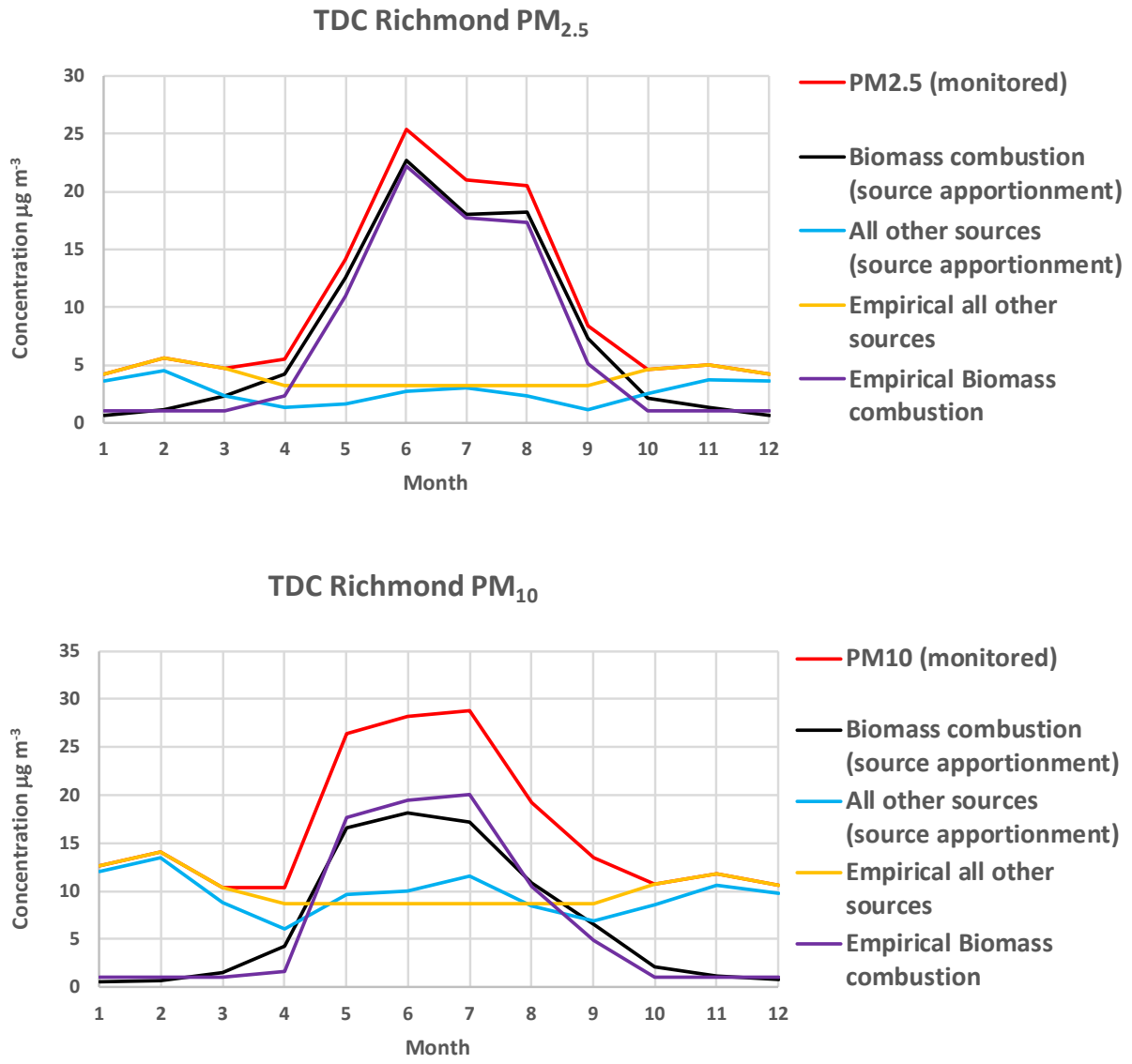

Figure 3.3 Empirical model performance for estimating monthly average Biomass combustion source contributions to (a) $PM_{2.5}$ (2016) and (b) PM_{10} (2013 to 2016) at Richmond, Tasman District showing peak winter concentrations.

The Richmond data presented in Figure 3.3 are the monthly averages for one year (2016) of $PM_{2.5}$ monitoring and three years (2013 to 2016) of PM_{10} monitoring. Figure 3.4 presents the scatterplot for the Richmond monthly data in Figure 3.3 showing good linear correlations between the empirical model and data derived from receptor modelling source apportionment analyses. Similar results to the Richmond case were obtained for the other 20 suitable $PM_{2.5}$ and PM_{10} speciation datasets used to compare the empirical model with observed data (see Section 3.2).

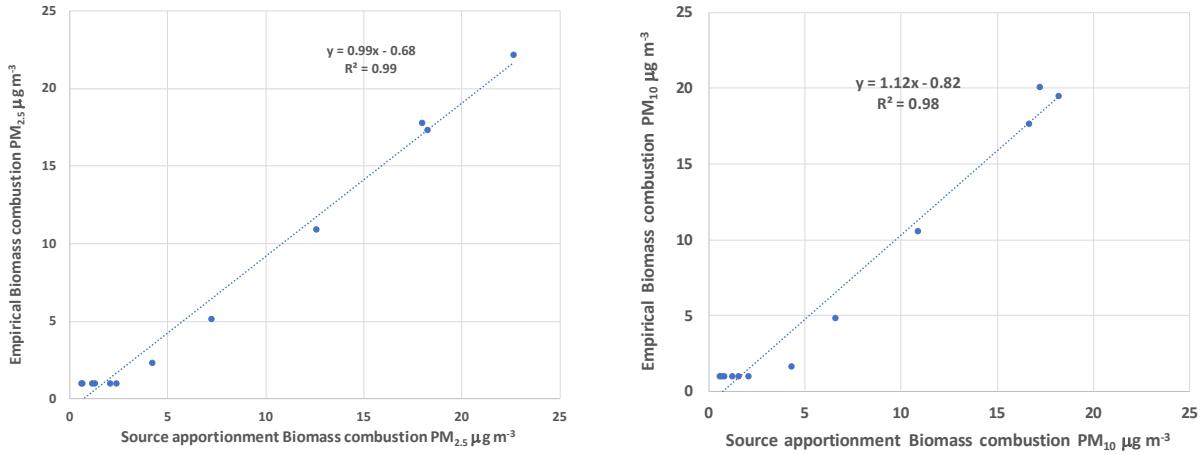

Figure 3.4 Linear comparison of the empirical model versus source apportionment data for monthly average Biomass combustion source contributions to (a) $PM_{2.5}$ (2016) and (b) PM_{10} (2013 to 2016) at Richmond, Tasman District.

3.1 Analyses of Sensitivity and Uncertainties in the Empirical Model

The empirical model was also compared to longer-term (i.e. multi-year data, where available) disaggregated monthly average data from source apportionment studies in order to understand interannual variations and the sensitivity of the empirical model to the estimated winter PM average without a biomass combustion peak.

Analyses of four years (2008 to 2012) of PM_{10} source apportionment data from Nelson (Ancelet et al. 2013, Ancelet et al. 2015) shows that the monthly average empirical model matches the source apportionment data for biomass combustion with good correlation as presented in Figure 3.5 and Figure 3.6. The red trace is the monitored PM data, while the black trace is the biomass combustion contribution from source apportionment. The light blue trace is the difference between these two quantities (i.e. the contribution from all other sources). The purple trace is the modelled biomass combustion contribution while the yellow trace is the modelled combination of natural and motor vehicle sources of particulate matter which can then be disaggregated further.

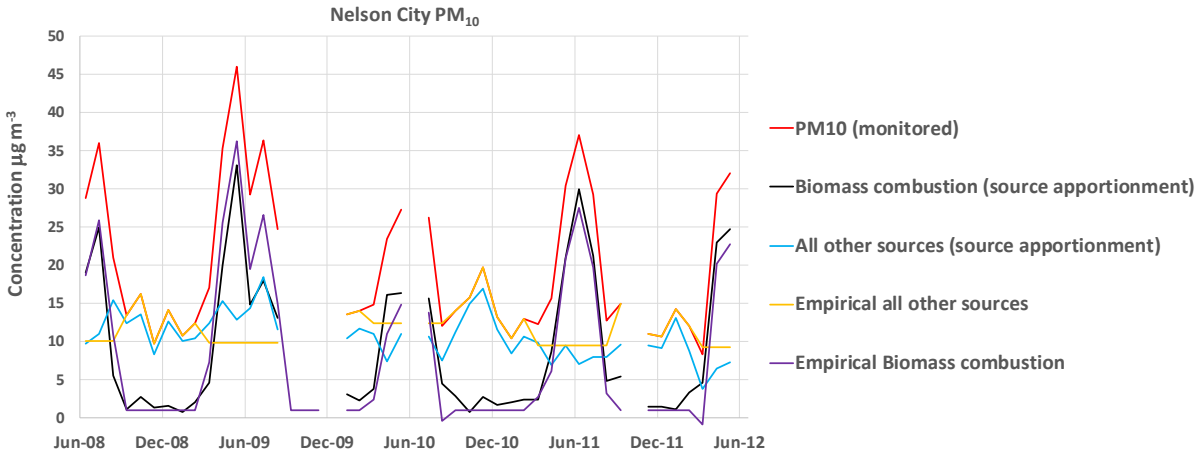

Figure 3.5 Empirical model for monthly average Biomass combustion source contributions to PM_{10} (2008 to 2012) at Nelson showing peak winter concentrations. Gaps in the data are due to missing sampling periods.

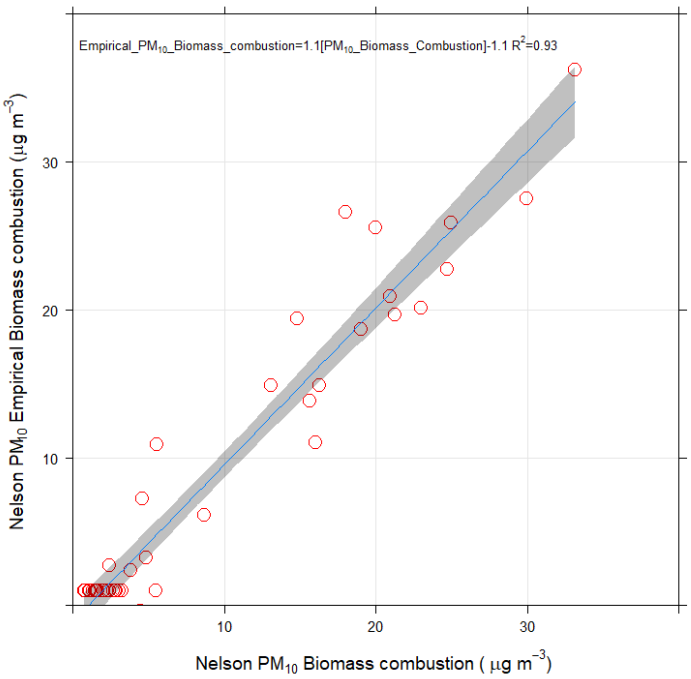

Figure 3.6 Linear comparison of the empirical model versus source apportionment data for monthly average Biomass combustion source contributions to PM_{10} (2008 to 2012) at Nelson.

It can be seen that there is some sensitivity for the empirical model to peaks in winter concentrations that are due to sources other than biomass combustion (light blue trace in Figure 3.5) since the model assumes that winter PM concentrations above the estimated average (i.e. with no biomass combustion) are all due to biomass combustion sources. However, the winter variation for other sources only has a minor effect on the modeled monthly averages if the winter biomass combustion peaks are relatively large compared to any contributions from those other sources, which is the case for most New Zealand urban areas during winter.

Analysis of data from a denser urban area in the northern half of the North Island (Takapuna in Auckland City) provided the opportunity to examine how the empirical model performs when the biomass combustion peak in winter is much smaller than that found for urban areas further south. The Takapuna data is part of a multi-site, multi-year source apportionment dataset for Auckland City (Davy and Trompetter 2018) that provides information on the impact and long-term trends for sources of particulate matter across the Auckland urban area. Similar to the Nelson case, Figure 3.7 presents the source apportionment and empirical model data for Takapuna $PM_{2.5}$ (2007 to June 2016) and PM_{10} (2006 to 2019).

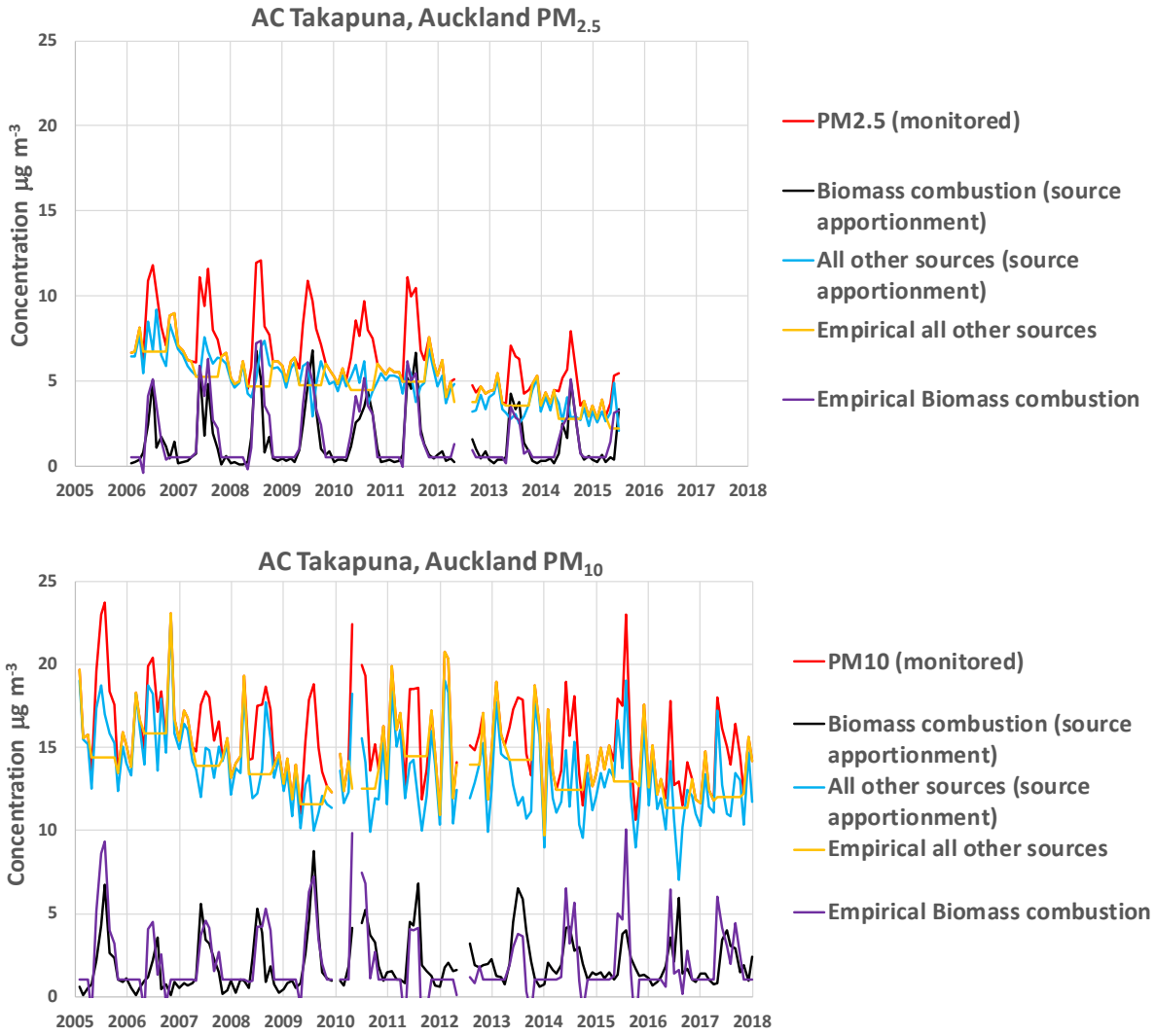

Figure 3.7 Empirical model for monthly average Biomass combustion source contributions to (a) $PM_{2.5}$ (2007 to 2016) and (b) PM_{10} (2006 to 2019) at Takapuna, Auckland showing peak winter concentrations. Gaps in the data are due to missing sampling periods.

Several features are evident in the data presented in Figure 3.7. Firstly, the winter peaks in $PM_{2.5}$ and PM_{10} concentrations are still evident but biomass combustion is not the dominant source overall (i.e. biomass concentrations are lower than the contributions from all other sources (as indicated by the light blue trace), more so for PM_{10} concentrations. The effect of this is to introduce more scatter (uncertainty) around the empirical estimate compared to the source apportionment values as shown in Figure 3.8 (b) for the PM_{10} data. The empirical estimate of biomass combustion contributions from $PM_{2.5}$ data (Figure 3.8 (a)) performs significantly better which is expected since particulate matter emissions from biomass combustion sources are generally within the $PM_{2.5}$ size fraction. The month to month variation in winter averages for coarse particle ($PM_{10-2.5}$) sources (sea salt, road dust, construction) has a significant effect on the PM_{10} empirical biomass combustion estimation.

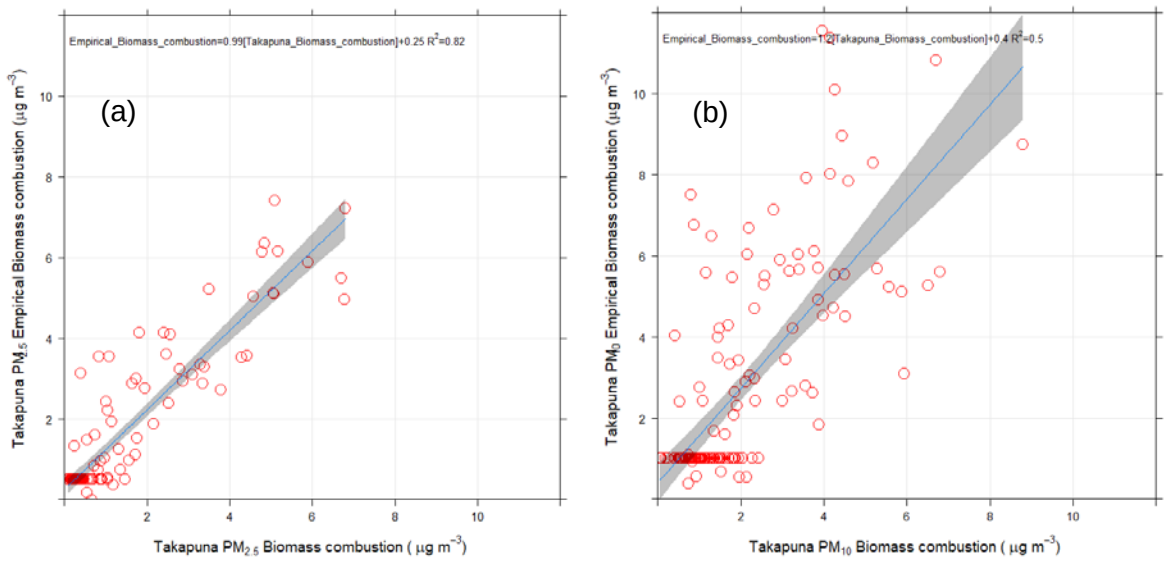

Figure 3.8 Linear comparison of the empirical model versus source apportionment data for monthly average Biomass combustion source contributions to (a) $PM_{2.5}$ (2007 to 2016) and (b) PM_{10} (2006 to 2019) at Takapuna, Auckland.

However, if several years of ensemble $PM_{2.5}$ or PM_{10} monthly averages are used to calculate the empirical biomass combustion value then this has the effect smoothing of the month to month variations in other sources as shown in Figure 3.9.

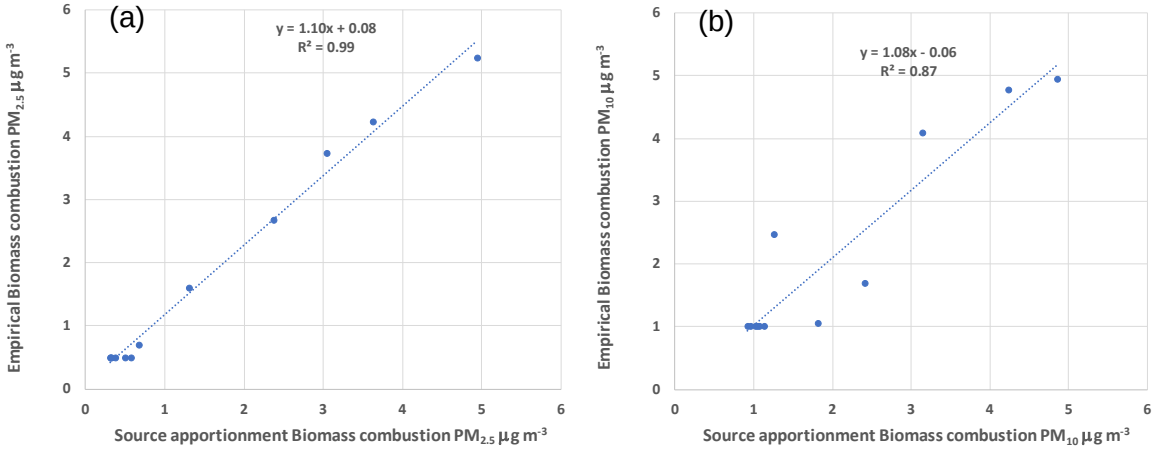

Figure 3.9 Linear comparison of the empirical model versus source apportionment data for ensemble monthly average Biomass combustion source contributions to (a) $PM_{2.5}$ (2007 to 2016) and (b) PM_{10} (2006 to 2019) at Takapuna, Auckland.

3.2 Summary Comparison Data for New Zealand Particulate Matter Speciation Monitoring Sites

The results from the empirical model indicate that the estimated average biomass combustion source contributions to total particulate matter concentrations are generally within 0.5 µg m^{-3} (average difference) of those derived from the respective source apportionment analyses as shown in Table 3.1 for $PM_{2.5}$ and Table 3.2 for PM_{10}.

Table 3.1 Comparison between Empirical Model and Source Apportionment contributions to $PM_{2.5}$.

Region	Site	Time period	$PM_{2.5}$	Source apportionment averages μg m^{-3}		Empirical model averages μg m^{-3}		Relative difference Biomass combustion	Relative difference All other sources
				Biomass combustion	All other sources	Empirical Biomass combustion	Empirical All other sources		
Wellington	Masterton	2002–2004	8.1	4.8	3.3	4.3	4.3	0.6	1.1
Wellington	Upper Hutt	2000–2002	4.8	2.1	2.7	3.2	2.1	1.1	0.6
Wellington	Wainuiomata	2006–2014	6.4	2.7	3.7	2.6	4.3	0.1	0.6
Wellington	Seaview	2005–2007	5.0	1.1	3.9	1.6	3.9	0.5	0.0
Wellington	Masterton East	2018	10.0	7.4	2.5	6.8	3.7	0.6	1.1
Auckland	Kingsland	2004–2007	7.1	2.4	4.7	2.7	4.4	0.3	0.3
Auckland	Takapuna	2007–2016	6.3	1.5	4.7	1.8	4.8	0.2	0.0
Auckland	Queen Street	2006–2016	8.7	0.7	8.0	1.0	7.7	0.3	0.3
Auckland	Penrose	2006–2016	7.0	1.7	5.3	1.8	5.2	0.1	0.1
Auckland	Khyber Pass Road	2006–2015	8.1	1.6	6.5	1.7	6.6	0.1	0.1
Auckland	Patumahoe	2010	3.4	0.9	2.5	0.7	2.9	0.2	0.4
Nelson	Nelson City	2006–2012	15.0	10.9	4.1	10.2	5.3	0.7	1.2
Otago	Dunedin	2010	10.4	4.0	6.5	2.5	8.7	1.5	2.3
Canterbury	Timaru	2006–2007	15.0	9.0	6.0	10.0	5.5	1.0	0.5
Canterbury	Woolston	2013–2014	9.5	3.2	6.3	4.2	5.8	1.0	0.5
Canterbury	Christchurch (Coles Place)	2013–2015	8.9	4.5	4.4	4.8	4.5	0.3	0.2
Hawkes Bay	Hastings	2006–2007	12.0	7.1	4.9	7.4	5.1	0.3	0.2

Region	Site	Time period	$PM_{2.5}$	Source apportionment averages μg m^{-3}		Empirical model averages μg m^{-3}		Relative difference Biomass combustion	Relative difference All other sources
				Biomass combustion	All other sources	Empirical Biomass combustion	Empirical All other sources		
Hawkes Bay	Awatoto	2016–2017	3.7	0.6	3.0	0.7	3.0	0.1	0.1
Hawkes Bay	Marewa Park	2017–2018	6.8	3.2	3.5	3.6	3.7	0.3	0.2
Waikato	Tokoroa	2015–2016	11.5	6.6	4.9	7.2	4.8	0.6	0.1
Tasman	Richmond	2015–2016	10.3	7.6	2.7	6.8	4.0	0.8	1.3

Table 3.2 Comparison between Empirical Model and Source Apportionment contributions to PM_{10}.

Region	Site	Time period	PM_{10}	Source apportionment averages μg m^{-3}		Empirical model averages μg m^{-3}		Relative difference Biomass combustion	Relative difference All other sources
				Biomass combustion	All other sources	Empirical Biomass combustion	Empirical All other sources		
Wellington	Masterton	2002–2004	16.4	6.2	10.3	5.8	11.1	0.4	0.9
Wellington	Upper Hutt	2000–2002	9.9	2.4	7.6	3.7	7.7	1.3	0.2
Wellington	Wainuiomata	2006–2014	13.4	3.0	10.4	2.7	11.2	0.3	0.8
Wellington	Seaview	2005–2007	16.4	1.1	15.4	1.5	15.5	0.4	0.1
Auckland	Kingsland	2004–2007	15.9	3.2	12.7	2.5	13.9	0.6	1.1
Auckland	Takapuna	2006–onwards	15.8	2.0	13.8	2.0	14.3	0.0	0.5
Auckland	Queen Street	2006–onwards	17.3	0.9	16.4	1.2	16.6	0.3	0.2
Auckland	Penrose	2006–2016	16.3	2.3	13.9	2.3	14.5	0.1	0.6
Auckland	Khyber Pass Road	2006–2015	18.0	1.5	16.6	1.7	16.8	0.2	0.3
Auckland	Henderson	2006–onwards	13.7	2.4	11.3	2.9	11.2	0.5	0.0
Auckland	Patumahoe	2010	10.9	0.9	10.0	0.9	10.5	0.0	0.5
Nelson	Tahunanui	2008–2009	20.6	7.3	13.4	6.1	15.0	1.1	1.6
Nelson	Nelson City	2006–2012	19.6	8.6	11.0	8.1	11.9	0.5	1.0
Otago	Dunedin	2010	27.3	4.0	23.3	3.8	23.5	0.1	0.2
Canterbury	Woolston	2013–2014	23.2	5.4	17.8	5.3	18.3	0.1	0.6
Canterbury	Christchurch (Coles Place)	2013–2015	19.4	4.9	14.5	4.1	15.6	0.7	1.1
Hawkes Bay	Awatoto	2016–2017	17.7	1.5	16.2	1.7	16.4	0.2	0.3
Hawkes Bay	Marewa Park	2017–2018	12.9	3.1	9.8	3.2	10.2	0.0	0.5

Region	Site	Time period	PM_{10}	Source apportionment averages μg m^{-3}		Empirical model averages μg m^{-3}		Relative difference Biomass combustion	Relative difference All other sources
				Biomass combustion	All other sources	Empirical Biomass combustion	Empirical All other sources		
Waikato	Tokoroa	2015–2016	14.0	5.8	8.2	5.7	8.8	0.2	0.7
Tasman	Richmond	2013–2016	16.4	6.7	9.7	6.7	10.2	0.0	0.5
Marlborough	Blenheim	2007	10.8	4.5	6.2	4.8	6.4	0.3	0.2

The empirical model was found to reproduce the peak winter contributions from biomass combustion (wood burning) for residential space heating with good linearity as shown in Figure 3.10 when compared to the source apportionment data for the same locations. The results are such that there is confidence the empirical model can be used to estimate annual average contributions to both $PM_{2.5}$ and PM_{10} from biomass combustion sources for use in health effects studies or assessing winter particulate matter concentration trends.

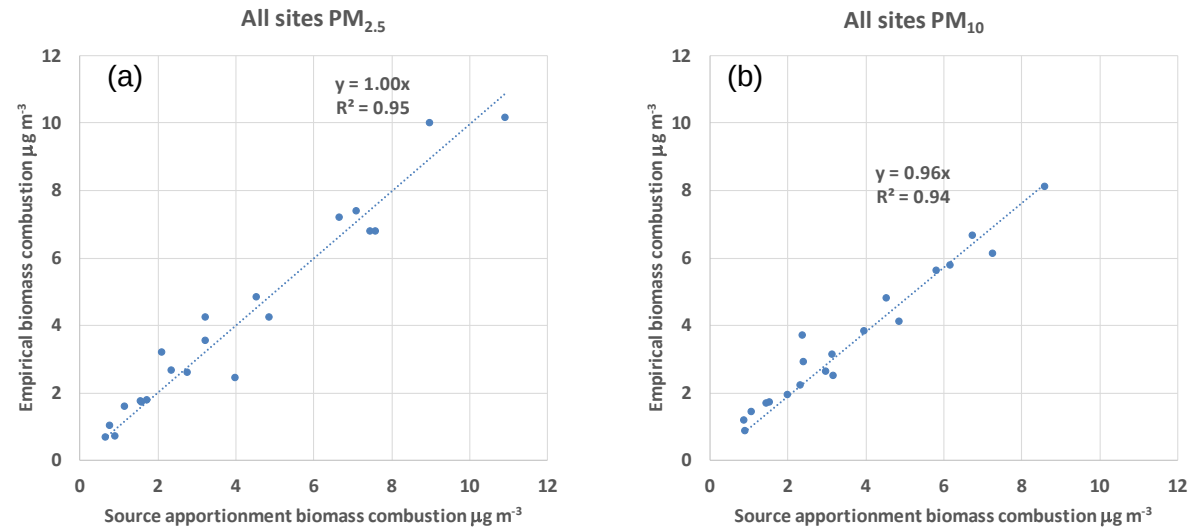

Figure 3.10 Linear comparison of the empirical model versus source apportionment data for average Biomass combustion source contributions to (a) $PM_{2.5}$ and (b) PM_{10} at all NZ sites.

3.3 Estimating Contributions from Other Sources to Urban Particulate Matter

While the empirical model described in the previous sections satisfactorily reproduces average biomass combustion concentrations it is also useful to approximate the contribution of other sources for exposure assessment when specific receptor modelling data is unavailable. The 'all other sources' component presented in Table 3.1 and Table 3.2 for $PM_{2.5}$ and PM_{10} respectively are the summed contributions from any source (other than biomass combustion) impacting at the monitoring site and Figure 3.11 presents this data graphically.

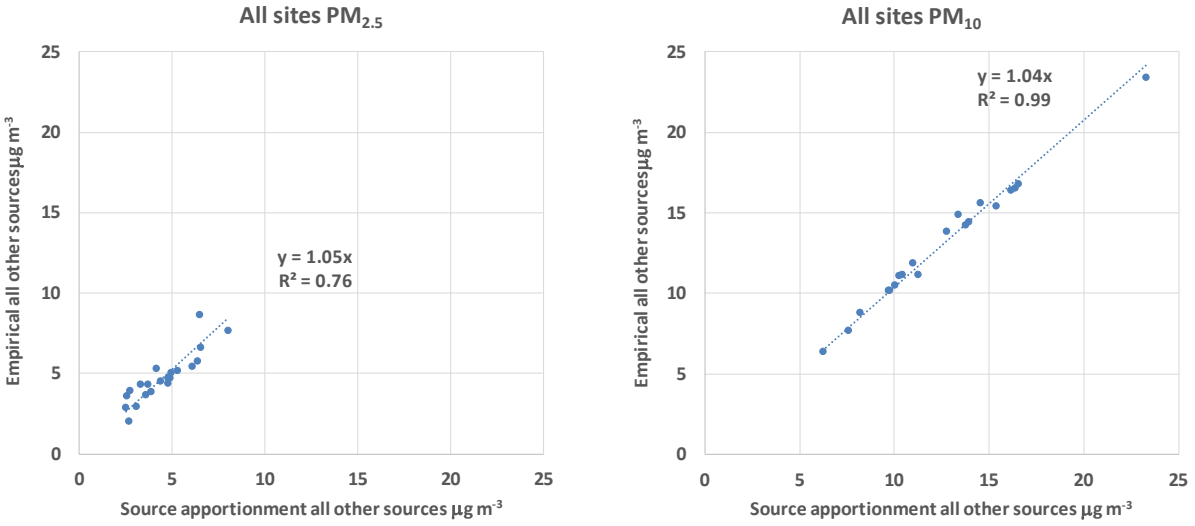

Figure 3.11 Linear comparison of the empirical model versus source apportionment data for average contributions from all other sources to (a) $PM_{2.5}$ and (b) PM_{10} at all NZ sites.

Interestingly Figure 3.11 shows that there is a significant coarse aerosol component to the 'all other sources' concentrations since $PM_{10} >> PM_{2.5}$. The 'all other source' $PM_{2.5}$ concentrations were largely due to motor vehicle tailpipe emissions and secondary sulphate along with small components of the marine aerosol and crustal matter sources since the latter two sources contribute primarily to the coarse particle ($PM_{10-2.5}$) size range.

3.3.1 Motor Vehicles and Crustal Matter

As discussed in Section 2.3, the contribution of motor vehicles to ambient particulate matter concentrations on an area basis (for exposure assessment) was likely to be influenced by the proximity to roadways, traffic volumes and density of the local urban roading network. Urban crustal matter (soil) contributions were also considered to be linked with motor vehicle activity. Metrics that capture vehicle activity such as VKT/km^2 or vehicle emissions/km^2 will also reflect the contribution of motor vehicles to ambient concentrations, both from tailpipe emissions and the associated road dust component. Such vehicle activity data can be compared to, and calibrated by, location specific receptor modelling results for motor vehicle source contributions to ambient particulate matter as presented in Table 3.3 and Table 3.4 for $PM_{2.5}$ and PM_{10} respectively. At a broader scale, the results for '*all other sources*' derived from the empirical model and presented in Table 3.1 and Table 3.2 could be used to give a measure of the motor vehicle influence (assuming that the crustal matter component is linked to motor vehicles) if the specific airshed increments for secondary sulphate and marine aerosol were first subtracted (see following sections). Another key feature of particulate matter attributed to motor vehicle activity from receptor modelling studies was that source contributions to ambient concentrations were higher on weekdays than on weekends and this reflects a similar pattern in traffic volumes.

Table 3.3 Average source contributions to $PM_{2.5}$ at sampling locations derived from receptor modelling analyses.

Region	Site	Period	$PM_{2.5}$	Biomass combustion	Motor vehicles	Secondary sulphate	Marine aerosol	Soil	Industry
Wellington	Masterton	2002–2004	9.28	6.08	0.40	0.55	0.62	0.73	
Wellington	Upper Hutt	2000–2002	5.40	2.36	1.36	0.81	0.37		
Wellington	Wainuiomata	2006–2014	6.64	2.64	0.79	1.22	1.69		
Wellington	Seaview	2005–2007	5.14	1.17	0.57	1.22	1.14	0.39	0.52
Wellington	Masterton East	2018	10.11	7.44	0.44	1.34	1.03		0.09
Auckland	Kingsland	2004–2007	7.12	2.20	1.92	0.76	1.26		
Auckland	Takapuna	2007–2016	6.50	1.52	1.82	0.89	2.20	0.13	
Auckland	Queen Street	2006–2016	8.76	0.76	4.23	1.00	1.81	0.13	0.50
Auckland	Penrose	2006–2016	7.05	1.77	2.34	0.79	0.56	0.38	0.23
Auckland	Khyber Pass Road	2006–2015	8.11	1.61	4.05	0.91	1.20	0.14	
Auckland	Patumahoe	2010	3.34	0.91		1.03	0.93	0.20	
Nelson	Nelson City	2006–2012	16.03	12.41	0.78	0.92	1.12	0.81	
Otago	Dunedin	2010	10.29	4.02	2.84	1.73	1.13		
Canterbury	Timaru	2006–2007	16.12	8.70	0.88	0.65	0.68		
Canterbury	Woolston	2013–2014	10.26	3.86	2.59	1.18	0.44	0.32	
Canterbury	Christchurch (Coles Place)	2013–2015	8.73	4.32	1.01	1.02	1.74	0.30	
Hawkes Bay	Hastings	2006–2007	11.75	6.90	1.11	1.22	1.26		
Hawkes Bay	Awatoto	2016–2017	3.75	0.70	0.20	0.80	1.20	0.10	0.30
Hawkes Bay	Marewa Park	2017–2018	6.80	3.19	0.15	1.29	1.20		0.34
Waikato	Tokoroa	2015–016	10.12	4.91	0.67	0.87	1.72	0.41	
Tasman	Richmond	2015–2016	10.57	7.79	0.38	0.86	1.25		0.08

Table 3.4 Average source contributions to PM_{10} at sampling locations derived from receptor modelling analyses.

Region	Site	Period	PM_{10}	Biomass combustion	Motor vehicles	Secondary sulphate	Marine aerosol	Soil	Industry
Wellington	Masterton	2002–2004	17.51	6.17	0.98	0.72	4.27	3.10	
Wellington	Upper Hutt	2000–2002	9.90	2.10	1.48	1.20	3.53	2.02	
Wellington	Wainuiomata	2006–2014	13.44	3.61	1.63	1.10	5.06	1.36	
Wellington	Seaview	2005–2007	16.60	1.03	2.22	2.62	6.38	3.20	0.53
Auckland	Kingsland	2004–2007	16.11	3.54	3.17	1.41	6.33	1.04	
Auckland	Takapuna	2006–onwards	15.56	1.97	3.59	1.66	6.39	0.63	0.34
Auckland	Queen Street	2006–onwards	17.45	0.89	6.41	0.87	7.38	0.65	0.54
Auckland	Penrose	2006–2016	16.50	2.40	4.11	1.09	6.64	0.54	0.97
Auckland	Khyber Pass Road	2006–2015	17.83	1.49	6.18	1.54	7.44	1.29	0.28
Auckland	Henderson	2006–onwards	13.79	2.44	1.94	1.41	6.80	0.80	0.15
Auckland	Patumahoe	2010	10.54	0.92		0.99	5.31	2.32	0.43
Nelson	Tahunanui	2008–2009	19.95	5.87	2.30	1.29	4.20	3.45	2.49
Nelson	Nelson City	2006–2012	20.41	9.75	2.02	2.11	3.72	2.65	
Otago	Dunedin	2010	26.87	4.02	2.84	1.73	4.86	7.45	5.10
Canterbury	Christchurch (Coles Place)	2013–2015	19.48	4.65	2.19	2.31	6.85	2.74	
Hawkes Bay	Awatoto	2016–2017	13.59	1.52	0.87	1.38	9.09	2.84	1.13
Hawkes Bay	Marewa Park	2017–2018	13.08	3.15	1.92	2.11	4.50		0.76
Waikato	Tokoroa	2015–2016	13.05	4.32	1.51	1.32	3.90	0.86	
Tasman	Richmond	2013–2016	17.08	7.57	3.64	2.08	2.93		0.14
Marlborough	Blenheim	2007	10.75	6.54	1.14	1.00	2.01	1.29	

3.3.2 Secondary Sulphate

Annual average secondary sulphate contributions to $PM_{2.5}$ were found to be reasonably uniform across the receptor modelling studies for New Zealand locations ranging from 0.6 to 1.7 µg m^{-3} as shown in Table 3.3. This most likely reflects the general influence of oceanic generated secondary sulphate across the country, with higher concentrations at locations that may be influenced by industrial emissions, near ports that have vessels using sulphur containing fuels, or by geothermal emissions of precursor gases (SO_2, H_2S). A $PM_{2.5}$ concentration increment of 1.0 µg m^{-3} as an annual average would be a reasonable estimate for the general population exposure to secondary sulphate aerosol across New Zealand.

3.3.3 Marine Aerosol

Marine aerosol (sea salt) is ubiquitous across New Zealand with all speciation monitoring sites sampling a clear signal, including inland locations such as Alexandra (Ancelet et al. 2014a) in Central Otago and Tokoroa (Davy and Trompetter 2017a) in the central North Island. Multi-site monitoring results within the same or adjacent airsheds has shown that marine aerosol concentrations can be uniform across a wide area (as discussed in Section 2.3.3.1). Therefore, the use of source apportionment derived marine aerosol contributions from a single site representative of a wider region will also be representative of population exposure in that region. The most significant factor affecting marine aerosol concentrations appears to be the degree to which a particular area is topographically sheltered from the northwest to southwesterly sweep of air masses from the Tasman Sea and Southern Ocean.

4.0 CONCLUSION

The analysis of source mass contributions to ambient particulate matter concentrations derived from receptor modelling has shown that an empirical model can be used to extract source information from $PM_{2.5}$ and PM_{10} monthly average concentration data. The empirical model has been demonstrated to robustly determine the contribution of biomass combustion sources (primarily wood burning for residential space heating) on a monthly or annual basis by exploiting the observed winter concentration peak from this source. Applications for the empirical model include exposure assessment for urban populations to determine the relative health impacts by particulate matter source or use for the trend analysis of peak winter particulate matter concentrations.

4.1 Further Work

Differentiating sources of airborne particulate matter is a complex mixture resolution problem usually approached by the collection of time-integrated atmospheric samples for compositional analyses and subsequent data science processing. Information on the sources responsible for air pollution is key to the attribution of health impacts and to implement effective management and mitigation strategies. While such monitoring campaigns can be resource intensive and take several years of data collection to resolve the contributing sources, they still remain a 'gold standard' for identifying the source(s) responsible for exceedances of the NESAQ PM_{10} standard (50 μm^{-3} 24-hour average).

It may be possible to extract further source information from routine monitoring data with more sophisticated data processing (such as a cognitive computing/machine learning approach) trained by our observational knowledge of diurnal, weekly and seasonal temporal patterns exhibited by different source categories, particularly for the influence of motor vehicle emissions on urban air quality.

5.0 ACKNOWLEDGMENTS

Auckland Council, Environment Waikato, Hawkes Bay Regional Council, Greater Wellington Regional Council, Marlborough District Council, Nelson City Council, Tasman District Council, Environment Canterbury, Otago Regional Council.

6.0 REFERENCES

Ancelet T, Davy PK, Mitchell T, Trompetter WJ, Markwitz A, Weatherburn DC. 2012. Identification of particulate matter sources on an hourly time-scale in a wood burning community. *Environmental Science and Technology*. 46(9):4767-4774. doi:10.1021/es203937y.

Ancelet T, Davy PK, Trompetter WJ. 2013. Source apportionment of PM_{10} and $PM_{2.5}$ in Nelson Airshed A. Lower Hutt (NZ): GNS Science. 95 p. Consultancy Report 2013/146. Prepared for Nelson City Council.

Ancelet T, Davy PK, Trompetter WJ. 2015. Particulate matter sources and long-term trends in a small New Zealand city. *Atmospheric Pollution Research*. 6(6):1105-1112. doi:10.1016/j.apr.2015.06.008.

Ancelet T, Davy PK, Trompetter WJ, Markwitz A, Weatherburn DC. 2010. A comparison of particulate and particle-phase PAH emissions from a modern wood burner with those of an old wood burner. *Air Quality and Climate Change*. 44:21-24.

Ancelet T, Davy PK, Trompetter WJ, Markwitz A, Weatherburn DC. 2011a. Carbonaceous aerosols in an urban tunnel. *Atmospheric Environment*. 45(26):4463-4469. doi:10.1016/j.atmosenv.2011.05.032.

Ancelet T, Davy PK, Trompetter WJ, Markwitz A, Weatherburn DC. 2011b. Characterisation of particulate matter emissions from a modern wood burner under varying burner conditions. *Air Quality and Climate Change*. 45(2):21-27.

Ancelet T, Davy PK, Trompetter WJ, Markwitz A, Weatherburn DC. 2014a. Particulate matter sources on an hourly timescale in a rural community during the winter. *Journal of the Air and Waste Management Association*. 64(5):501-508. doi:10.1080/10962247.2013.813414.

Ancelet T, Davy PK, Trompetter WJ, Markwitz A, Weatherburn DC. 2014b. Sources and transport of particulate matter on an hourly time-scale during the winter in a New Zealand urban valley. *Urban Climate*. 10:644-655. doi:10.1016/j.uclim.2014.06.003.

Bond TC, Bergstrom RW. 2006. Light absorption by carbonaceous particles : an investigative review. *Aerosol Science and Technology*. 40(1):27-67. doi:10.1080/02786820500421521.

Cohen DD. 1998. Characterisation of atmospheric fine particles using IBA techniques. *Nuclear Instruments and Methods in Physics Research Section B: Beam Interactions with Materials and Atoms*. 136-138:14-22. doi:10.1016/S0168-583X(97)00658-7.

Cohen DD, Bailey GM, Kondepudi R. 1996. Elemental analysis by PIXE and other IBA techniques and their application to source fingerprinting of atmospheric fine particle pollution. *Nuclear Instruments and Methods in Physics Research Section B: Beam Interactions with Materials and Atoms*. 109-110:218-226. doi:10.1016/0168-583X(95)00912-4.

Cohen D, Taha G, Stelcer E, Garton D, Box G. 2000. The measurement and sources of fine particle elemental carbon at several key sites in NSW over the past eight years. In. *Proceedings of the 15th International Clean Air and Environment Conference*. 2000 Nov 26-30; Sydney, Australia. Mooroolbark (AU): Clean Air Society of Australia and New Zealand.

Cohen D. 1999. Accelerator based ion beam techniques for trace element aerosol analysis. In: Landsberger S, Creatchman M, editors. *Elemental analysis of airborne particles*. Amsterdam (NL): Gordon and Breach Science Publishers. p. 139–196. (Advances in environmental, industrial, and process control technologies; 1).

Davy PK, Ancelet T, Trompetter WJ. 2016. Source apportionment of $PM_{2.5}$ and $PM_{10\text{-}2.5}$ samples from St Albans, Christchurch. Lower Hutt (NZ): GNS Science. 61 p. Consultancy Report 2016/72. Prepared for Environment Canterbury.

Davy PK, Trompetter WJ. 2017a. Source apportionment of $PM_{2.5}$ and PM_{10} sources in the Richmond airshed, Tasman District. GNS Science. 69 p. Consultancy Report 2017/86. Prepared for Tasman District Council.

Davy PK, Trompetter WJ. 2017b. Black carbon in New Zealand. Lower Hutt (NZ): GNS Science. 71 p. Consultancy Report 2017/22. Prepared for Ministry for the Environment.

Davy PK, Trompetter WJ. 2018. Heavy metals, black carbon and natural sources of particulate matter in New Zealand. Lower Hutt (NZ): GNS Science. 81 p. Consultancy Report 2017/238. Prepared for Ministry for the Environment.

Davy PK, Trompetter WJ. 2019. Composition, sources and long-term trends for Auckland air particulate matter: summary report. Lower Hutt (NZ): GNS Science. Consultancy Report 2019/151. Prepared for Auckland Council.

Davy PK, Trompetter WJ, Markwitz A. 2011a. Concentration, composition and sources of particulate matter in the Johnstone's Hill Tunnel, Auckland. Lower Hutt (NZ): GNS Science. 64 p. Consultancy Report 2010/296. Prepared for New Zealand Transport Agency.

Davy PK, Trompetter WJ, Markwitz A. 2009. Elemental analysis of wood burner emissions. GNS Science. 38 p. Consultancy Report 2009/258. Prepared for Auckland Regional Council.

Davy PK, Trompetter WJ, Markwitz A. 2011b. Source apportionment of airborne particles in the Auckland region: 2010 analysis. Lower Hutt (NZ): GNS Science. 324 p. Consultancy Report 2010/262. Prepared for Auckland Council.

Fine PM, Cass GR, Simoneit BRT. 2001. Chemical characterization of fine particle emissions from fireplace combustion of woods grown in the northeastern United States. *Environmental Science & Technology*. 35(13):2665-2675. doi:10.1021/es001466k.

Fitzgerald JW. 1991. Marine aerosols: a review. *Atmospheric Environment Part A General Topics*. 25(3):533–545. doi:10.1016/0960-1686(91)90050-H.

Hopke PK. 1999. An introduction to source receptor modeling. In: Landsberger S, Creatchman M, editors. *Elemental analysis of airborne particles*. Amsterdam (NL): Gordon and Breach Science Publishers.

Hopke PK, Xie Y, Paatero P. 1999. Mixed multiway analysis of airborne particle composition data. *Journal of Chemometrics*. 13(3-4):343-352. doi:10.1002/(SICI)1099-128X(199905/08)13:3/4<343::AID-CEM550>3.0.CO;2-P.

Horvath H. 1993. Atmospheric light absorption: a review. *Atmospheric Environment Part A General Topics*. 27(3):293-317. doi:10.1016/0960-1686(93)90104-7.

Horvath H. 1997. Experimental calibration for aerosol light absorption measurements using the integrating plate method—Summary of the data. *Journal of Aerosol Science*. 28(7):1149-1161. doi:10.1016/S0021-8502(97)00007-4.

Hyslop NP, Trzepla K, Yatkin S, White WH, Ancelet T, Davy P, Butler O, Gerboles M, Kohl S, McWilliams A, et al. 2019. An inter-laboratory evaluation of new multi-element reference materials for atmospheric particulate matter measurements. *Aerosol Science and Technology*. 53(7):771–782. doi:10.1080/02786826.2019.1606413.

Jacobson MC, Hansson HC, Noone KJ, Charlson RJ. 2000. Organic atmospheric aerosols: review and state of the science. *Reviews of Geophysics*. 38(2):267-294. doi:10.1029/1998RG000045.

Kara M, Hopke P, Dumanoglu Y, Altiok H, Elbir T, Odabasi M, Bayram A. 2015. Characterization of PM using multiple site data in a heavily industrialized region of Turkey. *Aerosol and Air Quality Research*. 15(1):11-27. doi:10.4209/aaqr.2014.02.0039.

Landsberger S, Creatchman M. 1999. Elemental analysis of airborne particles. Amsterdam (NL): Gordon and Breach Science Publishers.

Lide DR. 1992. CRC handbook of chemistry and physics, 1992–1993. 73rd ed. Boca Raton (FL): CRC Press. 1 vol.

Maenhaut W, Malmqvist KG. 2001. Particle induced x-ray emission analysis. In: van Grieken R, Markowicz A, editors. *Handbook of X-ray spectrometry*. 2nd ed. Antwerp (BE): Marcel Dekker.

Maxwell JA, Campbell JL, Teesdale WJ. 1989. The Guelph PIXE software package. *Nuclear Instruments and Methods in Physics Research Section B: Beam Interactions with Materials and Atoms*. 43(2):218-230. doi:10.1016/0168-583X(89)90042-6.

Maxwell JA, Teesdale WJ, Campbell JL. 1995. The Guelph PIXE software package II. *Nuclear Instruments and Methods in Physics Research Section B: Beam Interactions with Materials and Atoms*. 95(3):407-421. doi:10.1016/0168-583X(94)00540-0.

Paatero P, Tapper U. 1994. Positive matrix factorization: A non-negative factor model with optimal utilization of error estimates of data values. *Environmetrics*. 5(2):111-126. doi:10.1002/env.3170050203.

Polissar AV, Hopke PK, Harris JM. 2001. Source regions for atmospheric aerosol measured at Barrow, Alaska. *Environmental Science & Technology*. 35(21):4214–4226. doi:10.1021/es0107529.

Salma I, Chi X, Maenhaut W. 2004. Elemental and organic carbon in urban canyon and background environments in Budapest, Hungary. *Atmospheric Environment*. 38(1):27-36. doi:10.1016/j.atmosenv.2003.09.047.

Seinfeld JH, Pandis SN. 2006. Atmospheric chemistry and physics: from air pollution to climate change. 2nd ed. Hoboken (NJ): John Wiley. 1203 p.

Thorpe A, Harrison RM. 2008. Sources and properties of non-exhaust particulate matter from road traffic: a review. *Science of The Total Environment*. 400(1-3):270–282. doi:10.1016/j.scitotenv.2008.06.007.

Trompetter WJ, Markwitz A, Davy PK. 2005. Air particulate research capability at the New Zealand Ion Beam Analysis Facility using PIXE and IBA techniques. *International Journal of PIXE*. 15(03n04):249-255. doi:10.1142/s0129083505000581.

Trompetter WJ. 2004. Ion Beam Analysis results of air particulate filters from the Wellington Regional Council. Lower Hutt (NZ): Institute of Geological & Nuclear Sciences. 17 p. Client Report 2004/24. Prepared for Wellington Regional Council.

Trompetter WJ, Davy PK. 2019. Indoor air quality in NZ homes and garages. Lower Hutt (NZ): GNS Science. 219 p. Consultancy Report 2018/44. Prepared for BRANZ.

Trompetter WJ, Davy PK. Air particulate research capability at the New Zealand Ion Beam Analysis facility using PIXE and IBA techniques. In: Markwitz A, Kennedy JV, chair. *5th International Symposium on BioPIXE, January 17-21, 2005, Wellington, New Zealand: programme and abstracts*. Lower Hutt (NZ): Institute of Geological & Nuclear Sciences.

Trompetter WJ, Davy PK, Markwitz A. 2010. Influence of environmental conditions on carbonaceous particle concentrations within New Zealand. *Journal of Aerosol Science*. 41(1):134-142. doi:10.1016/j.jaerosci.2009.11.003.

Watson JG, Chow JC, Frazier CA. 1999. X-ray fluorescence analysis of ambient air samples. In: Landsberger S, Creatchman M, editors. *Elemental analysis of airborne particles*. Amsterdam (NL): Gordon and Breach Science Publishers. p. 67-96. (Advances in environmental, industrial, and process control technologies; 1).

Watson JG, Zhu T, Chow JC, Engelbrecht J, Fujita EM, Wilson WE. 2002. Receptor modeling application framework for particle source apportionment. *Chemosphere*. 49(9):1093-1136. doi:10.1016/S0045-6535(02)00243-6.

Yatkin S, Trzepla K, Hyslop NP, White WH, Butler O, Ancelet T, Davy P, Gerboles M, Kohl SD, McWilliams A, et al. 2020. Comparison of a priori and interlaboratory-measurement-consensus approaches for value assignment of multi-element reference materials on PTFE filters. *Microchemical Journal*. 158:105225. doi:10.1016/j.microc.2020.105225.

APPENDICES

This page left intentionally blank.

APPENDIX 1 AIR PARTICULATE MATTER ANALYSIS TECHNIQUES

Black carbon (BC) has been studied extensively, but it is still not clear to what degree it is elemental carbon (EC (or graphitic) C(0)) or high molecular weight refractory weight organic species or a combination of both (Jacobson et al. 2000). Current literature suggests that BC is likely a combination of both, and that for combustion sources such as petrol and diesel fuelled vehicles and Biomass burning (wood burning, coal burning), EC and organic carbon compounds (OC) are the principle aerosol components emitted (Fine et al. 2001, Jacobson et al. 2000, Salma et al. 2004, Watson et al. 2002).

Determination of carbon (soot) on filters was performed by light reflection to provide the BC concentration. The absorption and reflection of visible light on particles in the atmosphere or collected on filters is dependent on the particle concentration, density, refractive index and size. For atmospheric particles, BC is the most highly absorbing component in the visible light spectrum with very much smaller components coming from soils, sulphates and nitrate (Horvath1993, Horvath 1997). Hence, to the first order it can be assumed that all the absorption on atmospheric filters is due to BC. The main sources of atmospheric BC are anthropogenic combustion sources and include biomass burning, motor vehicles and industrial emissions (Cohen et al. 2000). Cohen and co-workers found that BC is typically 10–40% of the fine mass ($PM_{2.5}$) fraction in many urban areas of Australia.

When measuring BC by light reflection/transmission, light from a light source is transmitted through a filter onto a photocell. The amount of light absorption is proportional to the amount of black carbon present and provides a value that is a measure of the black carbon on the filter. Conversion of the absorbance value to an atmospheric concentration value of BC requires the use of an empirically derived equation (Cohen et al. 2000):

$$BC\ (\mu g\ cm^{-2}) = (100/2(F\varepsilon))\ \ln[R_0/R] \qquad A1.1$$

where:

ε is the mass absorbent coefficient for BC ($m^2\ g^{-1}$) at a given wavelength;

F is a correction factor to account for other absorbing factors such as sulphates, nitrates, shadowing and filter loading. These effects are generally assumed to be negligible and F is set at 1.00;

R_0, R are the pre- and post-reflection intensity measurements, respectively.

Black carbon was measured at GNS Science using the M43D Digital Smoke Stain Reflectometer. The following equation (from Willy Maenhaut, Institute for Nuclear Sciences, University of Gent Proeftuinstraat 86, B-9000 GENT, Belgium) was used for obtaining BC from reflectance measurements on Nucleopore polycarbonate filters or Pall Life Sciences Teflon filters:

$$BC\ (\mu g\ cm^{-2}) = [1000 \times LOG(R_{blank}/R_{sample}) + 2.39] / 45.8 \qquad A1.2$$

where:

R_{blank}:the average reflectance for a series of blank filters; R_{blank} is close (but not identical) to 100. GNS always use the same blank filter for adjusting to 100.

R_{sample}: the reflectance for a filter sample (normally lower than 100).

With: 2.39 and 45.8 constants derived using a series of 100 Nuclepore polycarbonate filter samples which served as secondary standards; the BC loading (in µg cm^{-2}) for these samples had been determined by Prof. Dr. M.O. Andreae (Max Planck Institute of Chemistry, Mainz, Germany) relative to standards that were prepared by collecting burning acetylene soot on filters and determining the mass concentration gravimetrically (Trompetter 2004).

A1.1 Elemental Concentrations by X-Ray Fluorescence Spectroscopy (XRF)

X-ray fluorescence spectroscopy (XRF) was used to measure elemental concentrations in $PM_{2.5}$ and $PM_{10-2.5}$ samples collected on polycarbonate filters at Awatoto. XRF measurements in this study were carried out at the GNS Science XRF facility and the spectrometer used was a PANalytical Epsilon 5 (PANalytical, the Netherlands). The Epsilon 5 is shown in Figure A1.1. XRF is a non-destructive and relatively rapid method for the elemental analysis of particulate matter samples.

Figure A1.1 The PANalytical Epsilon 5 spectrometer.

XRF is based on the measurement of characteristic X-rays produced by the ejection of an inner shell electron from an atom in the sample, creating a vacancy in the inner atomic shell. A higher energy electron then drops into the lower energy orbital and releases a fluorescent X-ray to remove excess energy (Watson et al. 1999). The energy of the released X-ray is characteristic of the emitting element and the area of the fluorescent X-ray peak (intensity of the peak) is proportional to the number of emitting atoms in the sample. From the intensity it is possible to calculate a specific element's concentration by direct comparison with standards.

To eject inner shell electrons from atoms in a sample, XRF spectrometer at GNS Science uses a 100 kV Sc/W X-ray tube. The 100 kV X-rays produced by this tube are able to provide elemental information for elements from Na–U. Unlike ion beam analysis techniques, which are similar to XRF, the PANalytical Epsilon 5 is able to use characteristic K-lines produced by each element for quantification. This is crucial for optimising limits of detection because K-lines have higher intensities and are located in less crowded regions of the X-ray spectrum. The X-rays emitted by the sample are detected using a high-performance Ge detector, which further improves the detection limits. Figure A1.2 presents a sample X-ray spectrum.

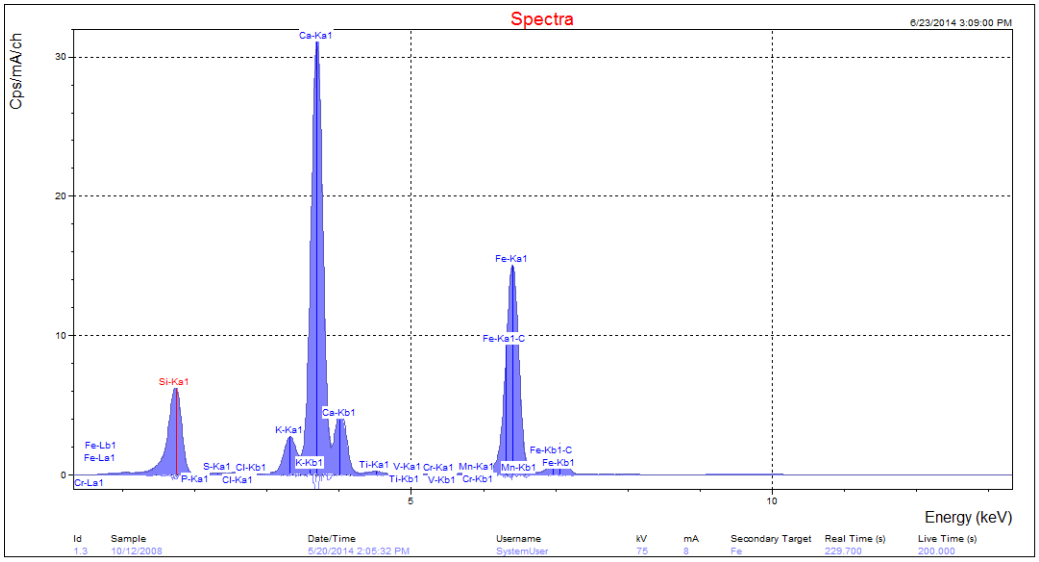

Figure A1.2 Example X-ray spectrum from a PM_{10} sample.

At GNS Science, calibration standards for each of the elements of interest were analysed prior to the samples being run. Once the calibration standards were analysed, spectral deconvolutions were performed using PANalytical software to correct for line overlaps and ensure that the spectra were accurately fit. Calibration curves for each element of interest were produced and used to determine the elemental concentrations from particulate matter samples. A NIST reference sample (SRM 2783) and multi-elemental reference standards from Crocker National Laboratory (University of California, Davis) were also analysed to ensure that the results obtained were robust and accurate.

A1.2 Elemental Concentrations by Ion Beam Analysis (IBA)

Ion beam analysis (IBA) was used to measure the elemental concentrations of particulate matter on the size-resolved filter samples from the Coles Place monitoring site. IBA is based on the measurement of characteristic X-rays and γ-rays of an element produced by ion-atom interactions using high-energy protons in the 2–5 million electron volt (MeV) range. IBA is a mature and well-developed science, with many research groups around the world using IBA in a variety of routine analytical applications, including the analysis of atmospheric aerosols (Maenhaut and Malmqvist 2001, Trompetter et al. 2005). IBA techniques do not require sample preparation and are fast, non-destructive and sensitive (Cohen 1999, Maenhaut and Malmqvist 2001, Trompetter et al. 2005).

IBA measurements for this study were carried out at the New Zealand IBA facility operated by GNS Science. Figure A1.3 shows the PM analysis chamber with its associated X-ray, γ-ray and particle detectors for Proton-Induced X-ray Emission (PIXE), Proton-Induced Gamma-ray

Emission (PIGE), Proton Elastic Scattering Analysis (PESA) and Rutherford Back Scattering (RBS) measurements.

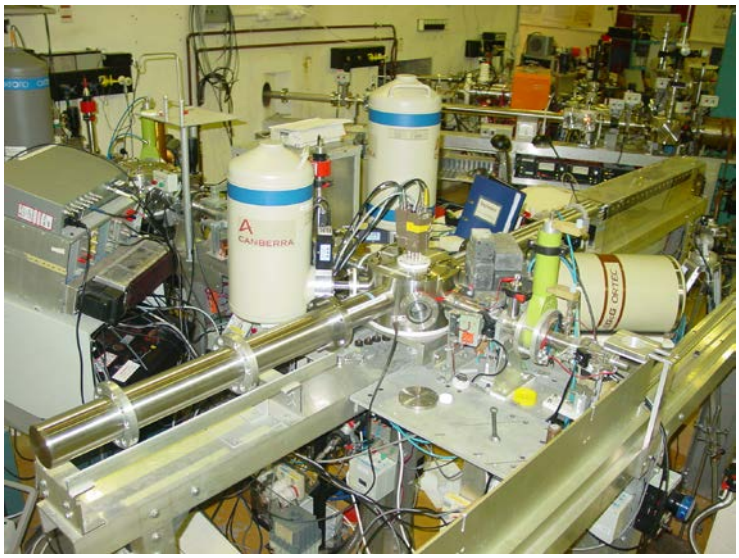

Figure A1.3 Particulate matter analysis chamber with its associated detectors.

The following sections provide a generalised overview of the IBA techniques used for elemental analysis and the analytical setup at GNS Science (Cohen 1998, Cohen et al. 1996, Trompetter 2004, Trompetter and Davy 2005). Figure A1.4 presents a schematic diagram of the typical experimental setup for IBA of air particulate filters at GNS Science.

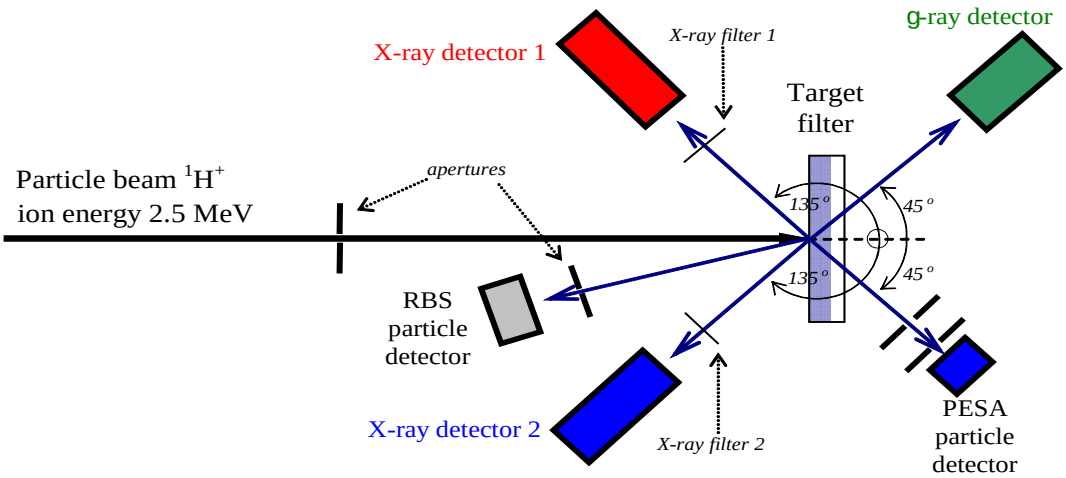

Figure A1.4 Schematic of the typical IBA experimental setup at GNS Science.

A1.2.1 Particle-Induced X-Ray Emission

Particle induced X-ray emission (PIXE), is used to determine elemental concentrations heavier than neon by exposing the filter samples to a proton beam accelerated to 2.5 million volts (MeV) by the GNS 3 MeV van-de-Graaff accelerator. When high energy protons interact with atoms in the sample, characteristic X-rays (from each element) are emitted by ion-electron processes. These X-rays are recorded in an energy spectrum. While all elements heavier than boron emit K X-rays, their production become too few to satisfactorily measure elements heavier than strontium. Elements heavier than strontium are detected via their lower energy L X-rays. The X-rays are detected using a Si(Li) detector and the pulses from the detector are amplified and

recorded in a pulse height analyser. In practice, sensitivities are further improved for the lighter elements by using two X-ray detectors, one for light element X-rays and the other for heavier element X-rays, each with different filtering and collimation. Figure A1.5 shows an example of a PIXE spectrum for airborne particles collected on a filter and analysed at the GNS IBA facility.

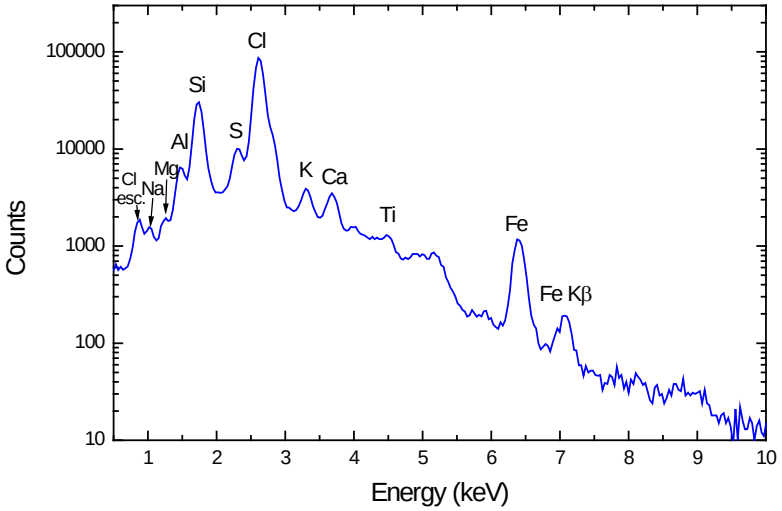

Figure A1.5 Typical PIXE spectrum for an aerosol sample analysed by PIXE.

As the PIXE spectrum consists of many peaks from different elements (and a Bremsstrahlung background), some of them overlapping, the spectrum is analysed with quantitative X-ray analysis software. In the case of this study, Gupix Software was used to perform the deconvolution with high accuracy (Maxwell et al. 1989, Maxwell et al. 1995). The number of pulses (counts) in each peak for a given element is used by the Gupix software to calculate the concentration of that element. The background and neighbouring elements determine the statistical error and the limit of detection. Note, that Gupix provides a specific statistical error and limit of detection (LOD) for each element in any filter, which is essential for source apportionment studies.

Typically, 20–25 elements from Mg–Pb are routinely determined above their respective LODs. Sodium (and fluorine) was determined using both PIXE and PIGE (see next section). Specific experimental details, where appropriate, are given in the results and analysis section.

A1.2.2 Particle-Induced Gamma-Ray Emission

Particle Induced Gamma-Ray Emission (PIGE) refers to γ-rays produced when an incident beam of protons interacts with the nuclei of an element in the sample (filter). During the de-excitation process, nuclei emit γ-ray photons of characteristic energies specific to each element. Typical elements measured with γ-ray are:

Element	*nuclear reaction*	*gamma ray energy (keV)*
Sodium	$^{23}Na(p,\alpha\gamma)^{20}Ne$	440, 1634
Fluorine	$^{19}F(p,\alpha\gamma)^{16}O$	197, 6129

Gamma rays are higher in energy than X-rays and are detected with a germanium detector. Measurements of a light element such as sodium can be measured more accurately using

PIGE because the γ-rays are not attenuated to the same extent in the filter matrix or the detector material, a problem in the measurement of low energy X-rays of sodium. Figure A1.6 shows a typical PIGE spectrum.

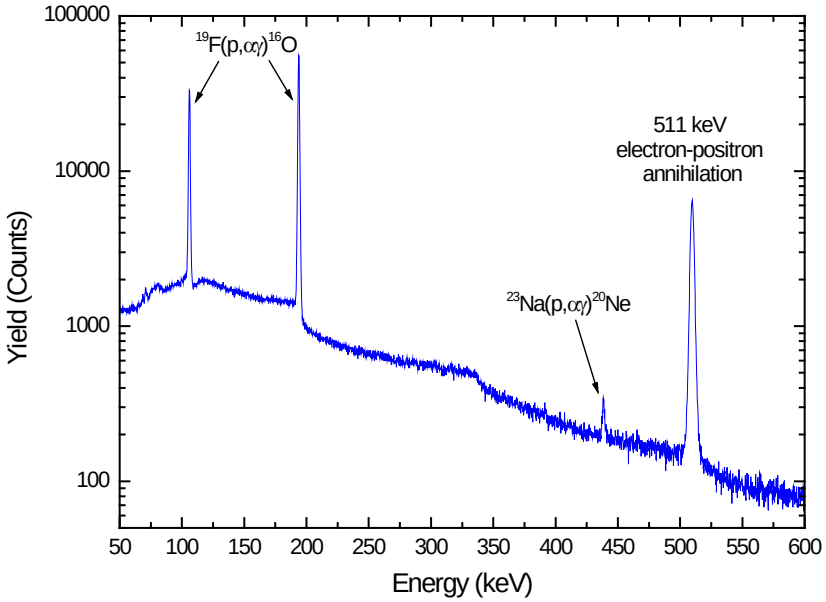

Figure A1.6 Typical PIGE spectrum for an aerosol sample.

A1.3 XRF and IBA Data Reporting

Most filters used to collect particulate matter samples for XRF or IBA analysis are sufficiently thin that the X-rays or ion beam penetrates the entire depth producing a quantitative analysis of elements present. Because of the thin nature of the air particulate matter filters, the concentrations reported from the analyses are therefore in aerial density units (ng cm^{-2}) and the total concentration of each element on the filters is calculated by multiplying with the exposed area of the filter. Typically, the exposed area is approximately 12 cm^2 for the sample deposit on the standard 47mm Teflon or polycarbonate filters used in most studies. For example, to convert from Cl (ng cm^{-2}) into Cl (ng m^{-3}) for filter samples, the equation is:

$$\text{Cl (ng m}^{-3}\text{)} = 11.95\ (\text{cm}^2) \times \text{Cl (ng cm}^{-2}\text{) / Vol(m}^3\text{)} \qquad \text{A1.3}$$

A1.3.1 Limits of detection and uncertainty reporting for elements

The exact limits of detection and associated analytical uncertainties for the concentration of each element depends on a number of factors such as:

- the method of detection;
- filter composition;
- sample composition;
- the detector resolution;
- spectral interference from other elements.

There are differences on how the analytical limits of detection (LOD) and uncertainties calculated between the XRF and IBA analytical methodologies due the nature of the measurements and the manner in which the sample spectra are deconvoluted by the associated software. Also, where and individual elemental concentration is reported as zero (0) means the measurement value (as derived from the spectral deconvolution) was zero but does not necessarily mean the element was not present but below the method limit of detection and indeterminate. Where this is the case then the corresponding uncertainty value (±) can be regarded as 5/6 LOD (Kara et al. 2015):

The following sections give an overview of this process for XRF and IBA respectively.

A1.3.1.1 Limits of detection and uncertainty reporting for elements determined by XRF

For XRF elemental data, the detection limits are defined in terms of the uncertainty in the blank (1σ) of 10 repeat measurements (USEPA Compendium Method IO-3.3). This ignores the effect of other elements which generally is small due to the use of multiple excitation frequencies except for the light elements (potassium and lower) where overlapping spectral lines will increase the detection limit.

Uncertainties for the XRF elemental data were calculated using the following equations (Kara et al. 2015):

$\sigma ij = xij + 2/3(DLj)$ for samples below limit of detection;

$\sigma ij = 0.2xij + 2/3(DLj)$; $DLj < xij < 3DLj$ and $\sigma ij = 0.1xij + 2/3(DLj)$; $xij > 3DLj$: for detected values

where xij is the determined concentration for species j in the ith sample, and DLj is the detection limit for species j.

A1.3.1.2 Limits of detection and uncertainty reporting for elements determined by IBA

For IBA, to determine the concentration of each element the background is subtracted, and peak areas fitted and calculated. The background occurs through energy loss, scattering and interactions of the ion beam as it passes through the filter material or from γ-rays produced in the target and scattered in the detector system (Cohen 1999). The peaks of elements in spectra that have interferences or backgrounds from other elements present in the air particulate matter, or filter matrix itself, will have higher limits of detection. The IBA was performed using a 3MeV accelerator proton beam with standards (SrF2, NaCl, Cr, Ni, SiO, KCl, Al) run before and after each analytical cycle. Spectral X-ray peak deconvolution was performed using Gupix software (Maxwell et al. 1989, 1995). The number of pulses (counts) in each peak for a given element is used by the Gupix software to calculate the concentration of that element. The background and neighbouring elements determine the statistical error and the limit of detection. Note that Gupix provides a specific statistical error (uncertainty) and limit of detection (LOD) for each element in each PM sample. The statistical uncertainty is calculated from the X-ray peak fitting process (called the fit error) and is related to the square root of the peak area. The limit of detection for an element in each sample spectra is defined as three times the error (3σ) obtained for the background and overlap (but not the elements own area) in a 1 full-width-half-maximum region centred about the principal X-ray peak of the element. The summary statistics provided for elemental concentrations in each dataset are therefore averages of the individual uncertainty and LOD values.

Choice of filter material is an important consideration with respect to elements of interest as is avoiding sources of contamination. The GNS IBA laboratory routinely runs filter blanks to correct for filter derived analytical artefacts as part of their QA/QC procedures. Figure A1.7 shows the LODs typically achieved by PIXE for each element at the GNS IBA facility. All IBA elemental concentrations determined in this work were accompanied by their respective LODs. The use of elemental LODs is important in receptor modeling applications.

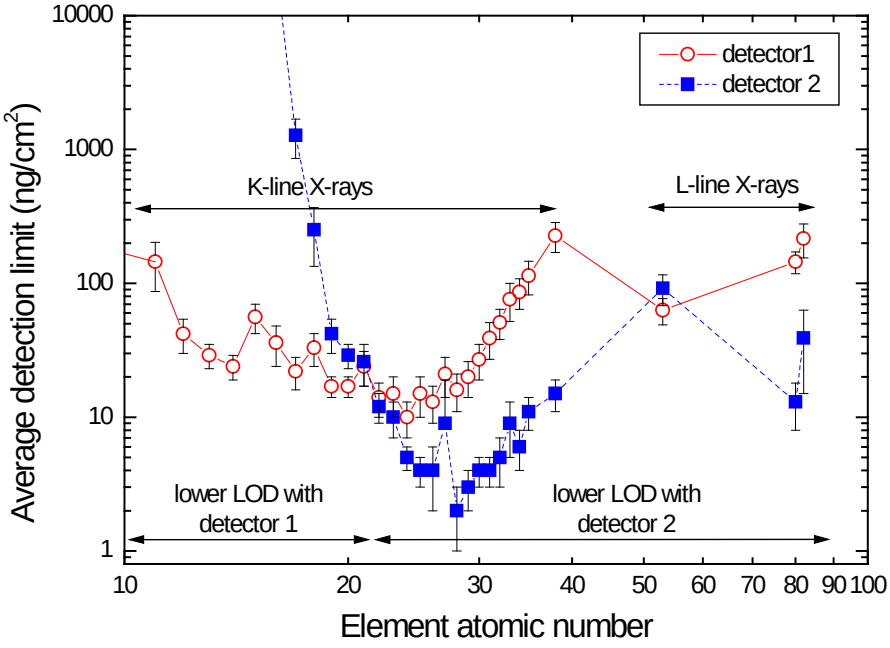

Figure A1.7 Elemental limits of detection for PIXE routinely achieved as the GNS IBA facility for air filters.

APPENDIX 2 NEW ZEALAND AIRPARTICULATE MATTER SAMPLING AND SPECIAITION SITES (TO 2020)

Location	Sites	Time period	Frequency	Size fraction	Location	Data owner	Quality comment
					Lat; Long (decimal degrees)		
Northland	Whangarei	2004–2012	1 day-in-6	PM10	-35.7252; 174.3177	NRC, GNS	Screening/trend
Wellington Region	Masterton	2002–2004	1 day-in-3,	PM2.5, PM10-2.5	-40.9523; 175.6465	GNS, GWRC	AQM
Wellington Region	Masterton (2 sites)	Winter 2010	Hourly	PM2.5, PM10-2.5	-40.9593; 175.6531	GNS	Research
Wellington Region	Upper Hutt	2000–2002	Variable	PM2.5, PM10-2.5	-41.1308; 175.0426	GNS, GWRC	Research
Wellington Region	Wainuiomata	2006–2008, 2011–2014	1 day-in-3	PM2.5, PM10-2.5	-41.2681; 174.9534	GWRC	AQM
Wellington Region	Wainuiomata	2014–onwards	6-hourly continuous	PM2.5, PM10-2.5	-41.2681; 174.9534	GWRC	AQM
Wellington Region	Seaview	2002–2004, 2005–2007	1 day-in-3	PM2.5, PM10-2.5	-41.2405; 174.9140	GWRC	AQM
Wellington Region	Wairarapa (Masterton, Carterton, Featherston)	Winter 2009	Daily (screening)	PM2.5, PM10-2.5		GWRC	Screening
Wellington Region	Mt Victoria Tunnel	Summer 2009		PM2.5, PM10-2.5	-41.3035; 174.7892	GNS	Research
Wellington Region	Baring Head	1996–1998		PM2.5, PM10-2.5	-41.4082; 174.8714	GNS	Research
Wellington Region	Raumati	Winter 2010	12-hourly	PM2.5, PM10-2.5	-40.9321; 174.9799	GWRC	AQM

Location	Sites	Time period	Frequency	Size fraction	Location	Data owner	Quality comment
					Lat; Long (decimal degrees)		
Wellington Region	7 Wellington sites indoor/outdoor	Winter 2017	2-hourly	PM2.5, PM10-2.5		GNS	Research
Wellington Region	Masterton East	2018	1-day-in-3	PM2.5	-40.9593; 175.6531	GWRC	AQM
Auckland Region	Kingsland	2004–2007	1 day-in-3	PM2.5, PM10	-36.8732; 174.7471	AC	AQM
Auckland Region	Takapuna	2007–2016	1 day-in-3	PM2.5	-36.7803; 174.7489	AC	AQM
Auckland Region	Takapuna	2006–onwards	1 day-in-3	PM10	-36.7803; 174.7489	AC	AQM
Auckland Region	Takapuna (3 sites)	Winter 2012	Hourly	PM2.5, PM10-2.5	-36.7803; 174.7489	GNS	AQM
Auckland Region	Queen Street	2006–2016	1 day-in-3	PM2.5	-36.8476;174.7655	AC	AQM
Auckland Region	Queen Street	2006–onwards	Daily	PM10	-36.8476; 174.7655	AC	AQM
Auckland Region	Penrose	2006–2016	1 day-in-3	PM2.5, PM10	-36.9045; 174.8156	AC	AQM
Auckland Region	Khyber Pass Road	2006–2015	1 day-in-3	PM2.5, PM10	-36.8662; 174.7705	AC	AQM
Auckland Region	Henderson	2006–onwards	1 day-in-3	PM10	-36.8681; 174.6284	AC	AQM
Auckland Region	Patumahoe	2010	Daily	PM2.5, PM10-2.5	-37.2046; 174.8639	AC	AQM

Location	Sites	Time period	Frequency	Size fraction	Location	Data owner	Quality comment
					Lat; Long (decimal degrees)		
Auckland Region	Johnstone Hills tunnel	Jun 2010	3-hourly	PM2.5, PM10-2.5	-36.5353; 174.6800	NZTA	Research
Nelson	Tahunanui	2008–2009	1 day-in-3	PM10	-41.2949; 173.2431	NCC	AQM
Nelson	Nelson City	2006–2012	1 day-in-6,	PM2.5, PM10	-41.1642; 173.1624	NCC	AQM
Nelson	Nelson City (3 sites)	Winter 2011	Hourly	PM2.5, PM10-2.5		GNS	Research
Marlborough	Blenheim	2007	1 day-in-3	PM2.5, PM10-2.5	-41.5268; 173.9561	MDC	AQM
Otago	Dunedin	2010	1 day-in-3	PM2.5, PM10-2.5	-45.8689; 170.5177	ORC	AQM
Otago	Alexandra (3 sites)	Winter 2011	Hourly	PM2.5, PM10-2.5	-45.2534; 169.3912	GNS	Research
Canterbury	Christchurch	2001–2002	Daily	PM2.5	-43.5112; 172.6337	ECAN	
Canterbury	Timaru	2006–2007	1 day-in-3	PM2.5	-44.4046; 171.2496	ECAN	
Canterbury	Woolston	2013–2014	2-hourly	PM2.5, PM10-2.5	-43.5572; 172.6811	ECAN/GNS	Research
Canterbury	Christchurch (Coles Place)	2013–2015	1 day-in-3	PM2.5, PM10-2.5	-43.5112; 172.6337	ECAN/GNS	AQM

Location	Sites	Time period	Frequency	Size fraction	Location	Data owner	Quality comment
					Lat; Long (decimal degrees)		
Canterbury	Christchurch (Coles Place, Woolston, Riccarton) high resolution 3-site study	Winter 2014	2-hourly	PM2.5, PM10-2.5	-43.5112; 172.6337	ECAN/GNS	Research
Hawkes Bay	Hastings	2006–2007	1 day-in-3	PM2.5, PM10	-39.6385; 176.8574	HBRC, NIWA, GNS	AQM
Hawkes Bay	Meanee Rd	2006+2008	1 day-in-2 (screening survey)			HBRC	Screening
Hawkes Bay	Napier	2008–2009	1 day-in-3	PM2.5, PM10-2.5		HBRC	
Hawkes Bay	Awatoto	2016–2017	1 day-in-3	PM2.5, PM10-2.5	-39.5459; 176.9192	HBRC/GNS	AQM
Hawkes Bay	Marewa Park	2017–2018	1 day-in-3	PM2.5, PM10-2.5	-39.5002; 176.8971	HBRC/GNS	AQM
Southland	Invercargill	Winter 2014	Hourly	PM2.5, PM10-2.5	-46.4305; 168.3711	SRC/GNS	AQM
Waikato	Tokoroa	Winter 2014	Daily	PM10	-38.2216; 175.8589	WRC/GNS	Screening
Waikato	Tokoroa	October 2015–October 2016	Daily	PM10	-38.2216; 175.8589	WRC/GNS	AQM
Bay of Plenty	Rotorua (Whakarewarewa Village)	October 2014–onwards	1 day-in-3	PM2.5, PM10-2.5	-38.1625; 176.2571	GNS	Research
Tasman	Richmond	2013–2016	1 day-in-3	PM10	-41.3396; 173.1833	TDC/GNS	AQM
Tasman	Richmond	2015–2016	Daily	PM2.5	-41.3396; 173.1833	TDC/GNS	AQM

Notes on quality comment

Screening	Qualitative analysis for identifying source types and/or sources contributing to ambient particulate matter, may be gaps in data, very short-term dataset or some sources may be significantly underestimated due to missing species - dataset considered incomplete for quantitative analysis
Research	Data used for research purposes, may not cover full seasonal or temporal variation
AQM	Data considered appropriate to use for air quality management purposes

APPENDIX 3 EMPIRICAL MODEL CALCULATION TEMPLATES

A3.1 $PM_{2.5}$ Empirical Model Calculation templates

Table A3.1 Empirical calculation template for $PM_{2.5}$ north of Bombay Hills

Month	Monthly average $PM_{2.5}$ (X) ($\mu g\ m^{-3}$)	Empirical All other source $PM_{2.5}$ (Y) ($\mu g\ m^{-3}$)	Empirical Biomass $PM_{2.5}$ (Z) ($\mu g\ m^{-3}$)
Jan	X1	Y1 = X1	Z1 = 0.50
Feb	X2	Y2 = X2	Z2 = 0.50
Mar	X3	Y3 = X3	Z3 = 0.50
Apr	X4	Y4 = AVERAGE(Y1:Y3,Y10:Y12)—1	Z4 = X4—Y4
May	X5	Y5 = AVERAGE(Y1:Y3,Y10:Y12)—1	Z5 = X5—Y5
Jun	X6	Y6 = AVERAGE(Y1:Y3,Y10:Y12)—1	Z6 = X6—Y6
Jul	X7	Y7 = AVERAGE(Y1:Y3,Y10:Y12)—1	Z7 = X7—Y7
Aug	X8	Y8 = AVERAGE(Y1:Y3,Y10:Y12)—1	Z8 = X8—Y8
Sep	X9	Y9 = AVERAGE(Y1:Y3,Y10:Y12)—1	Z9 = X9—Y9
Oct	X10	Y10 = X10	Z10 = 0.50
Nov	X11	Y11 = X11	Z11 = 0.50
Dec	X12	Y12 = X12	Z12 = 0.50
Average	$\overline{X}$	$\overline{Y}$	$\overline{Z}$

Table A3.2 Empirical calculation template for $PM_{2.5}$ south of Bombay Hills

Month	Monthly average $PM_{2.5}$ (X) ($\mu g\ m^{-3}$)	Empirical All other source $PM_{2.5}$ (Y) ($\mu g\ m^{-3}$)	Empirical Biomass $PM_{2.5}$ (Z) ($\mu g\ m^{-3}$)
Jan	X1	Y1 = X1	Z1 = 1.0
Feb	X2	Y2 = X2	Z2 = 1.0
Mar	X3	Y3 = X3	Z3 = 1.0
Apr	X4	Y4 = AVERAGE(Y1:Y3,Y10:Y12)—1.5	Z4 = X4—Y4
May	X5	Y5 = AVERAGE(Y1:Y3,Y10:Y12)—1.5	Z5 = X5—Y5
Jun	X6	Y6 = AVERAGE(Y1:Y3,Y10:Y12)—1.5	Z6 = X6—Y6
Jul	X7	Y7 = AVERAGE(Y1:Y3,Y10:Y12)—1.5	Z7 = X7—Y7
Aug	X8	Y8 = AVERAGE(Y1:Y3,Y10:Y12)—1.5	Z8 = X8—Y8
Sep	X9	Y9 = AVERAGE(Y1:Y3,Y10:Y12)—1.5	Z9 = X9—Y9

Month	Monthly average $PM_{2.5}$ (X) ($\mu g\ m^{-3}$)	Empirical All other source $PM_{2.5}$ (Y) ($\mu g\ m^{-3}$)	Empirical Biomass $PM_{2.5}$ (Z) ($\mu g\ m^{-3}$)
Oct	X10	Y10 = X10	Z10 = 1.0
Nov	X11	Y11 = X11	Z11 = 1.0
Dec	X12	Y12 = X12	Z12 = 1.0
Average	$\overline{X}$	$\overline{Y}$	$\overline{Z}$

A3.2 PM_{10} Empirical Model Calculation templates

Table A3.3 Empirical calculation template for PM_{10} north of Bombay Hills

Month	Monthly average PM_{10} (X) ($\mu g\ m^{-3}$)	Empirical All other source PM_{10} (Y) ($\mu g\ m^{-3}$)	Empirical Biomass PM_{10} (Z) ($\mu g\ m^{-3}$)
Jan	X1	Y1 = X1	Z1 = 1.0
Feb	X2	Y2 = X2	Z2 = 1.0
Mar	X3	Y3 = X3	Z3 = 1.0
Apr	X4	Y4 = AVERAGE(Y1:Y3,Y10:Y12)—1.5	Z4 = X4—Y4
May	X5	Y5 = AVERAGE(Y1:Y3,Y10:Y12)—1.5	Z5 = X5—Y5
Jun	X6	Y6 = AVERAGE(Y1:Y3,Y10:Y12)—1.5	Z6 = X6—Y6
Jul	X7	Y7 = AVERAGE(Y1:Y3,Y10:Y12)—1.5	Z7 = X7—Y7
Aug	X8	Y8 = AVERAGE(Y1:Y3,Y10:Y12)—1.5	Z8 = X8—Y8
Sep	X9	Y9 = AVERAGE(Y1:Y3,Y10:Y12)—1.5	Z9 = X9—Y9
Oct	X10	Y10 = X10	Z10 = 1.0
Nov	X11	Y11 = X11	Z11 = 1.0
Dec	X12	Y12 = X12	Z12 = 1.0
Average	$\overline{X}$	$\overline{Y}$	$\overline{Z}$

Table A3.4 Empirical calculation template for PM_{10} south of Bombay Hills

Month	Monthly average PM_{10} (X) ($\mu g\ m^{-3}$)	Empirical All other source PM_{10} (Y) ($\mu g\ m^{-3}$)	Empirical Biomass PM_{10} (Z) ($\mu g\ m^{-3}$)
Jan	X1	Y1 = X1	Z1 = 1.0
Feb	X2	Y2 = X2	Z2 = 1.0
Mar	X3	Y3 = X3	Z3 = 1.0
Apr	X4	Y4 = AVERAGE(Y1:Y3,Y10:Y12)—3	Z4 = X4—Y4
May	X5	Y5 = AVERAGE(Y1:Y3,Y10:Y12)—3	Z5 = X5—Y5
Jun	X6	Y6 = AVERAGE(Y1:Y3,Y10:Y12)—3	Z6 = X6—Y6
Jul	X7	Y7 = AVERAGE(Y1:Y3,Y10:Y12)—3	Z7 = X7—Y7
Aug	X8	Y8 = AVERAGE(Y1:Y3,Y10:Y12)—3	Z8 = X8—Y8
Sep	X9	Y9 = AVERAGE(Y1:Y3,Y10:Y12)—3	Z9 = X9—Y9
Oct	X10	Y10 = X10	Z10 = 1.0
Nov	X11	Y11 = X11	Z11 = 1.0
Dec	X12	Y12 = X12	Z12 = 1.0
Average	$\overline{X}$	$\overline{Y}$	$\overline{Z}$

www.gns.cri.nz

Principal Location

1 Fairway Drive, Avalon
Lower Hutt 5010
PO Box 30368
Lower Hutt 5040
New Zealand
T +64-4-570 1444
F +64-4-570 4600

Other Locations

Dunedin Research Centre
764 Cumberland Street
Private Bag 1930
Dunedin 9054
New Zealand
T +64-3-477 4050
F +64-3-477 5232

Wairakei Research Centre
114 Karetoto Road
Private Bag 2000
Taupo 3352
New Zealand
T +64-7-374 8211
F +64-7-374 8199

National Isotope Centre
30 Gracefield Road
PO Box 30368
Lower Hutt 5040
New Zealand
T +64-4-570 1444
F +64-4-570 4657